Space Science and Engineering Center
University of Wisconsin-Madison

An Investigation of the Utility of High Resolution Satellite Measured "Skin" Temperatures in Severe Weather Prediction and Diagnosis of Surface Characteristics

A REPORT from the

Cooperative Institute for Meteorological Satellite Studies

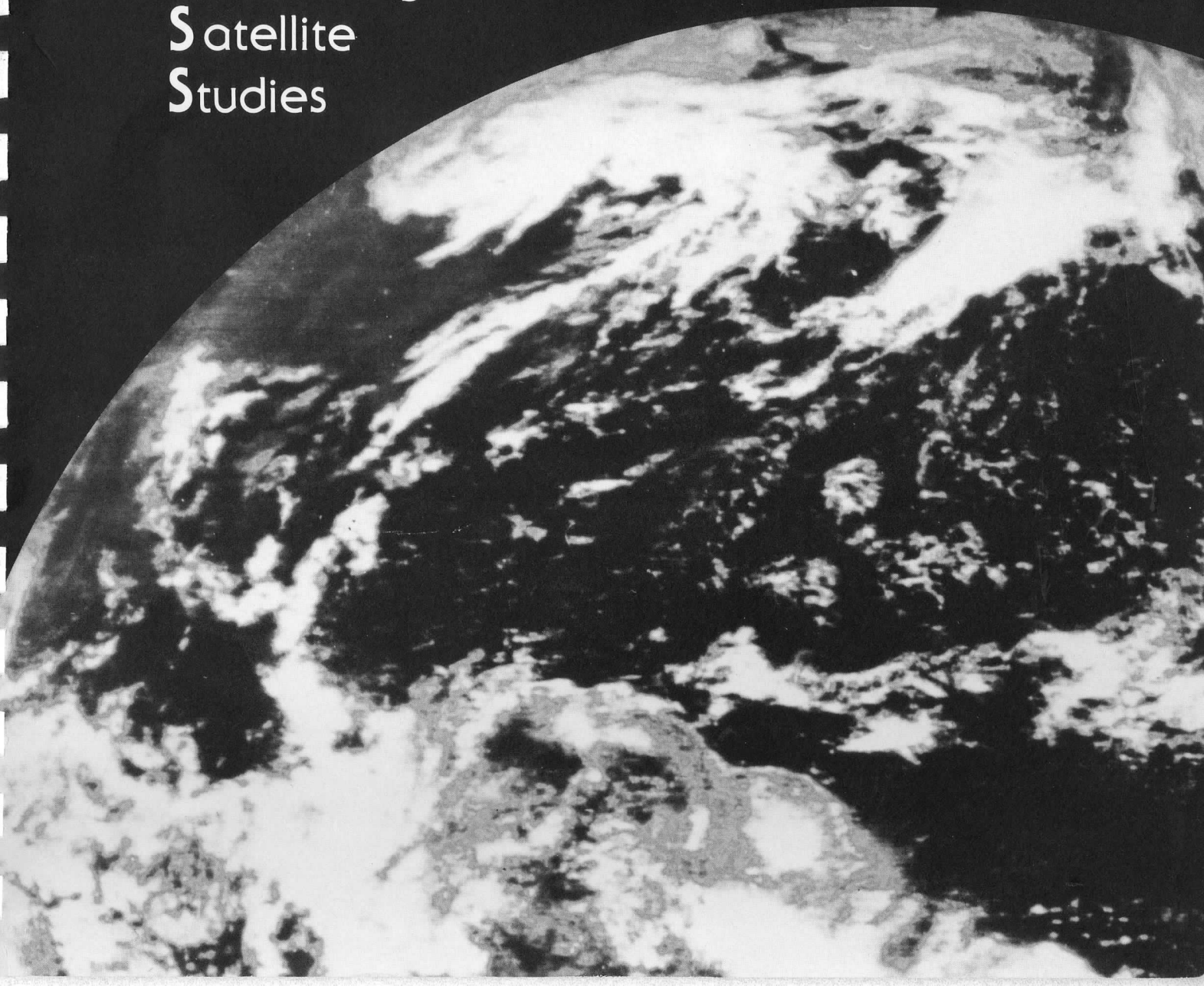

An Investigation of the Utility of High Resolution Satellite Measured "Skin" Temperatures in Severe Weather Prediction and Diagnosis of Surface Characteristics

A Report to

The National Science Foundation

for

Grant #ATM-8218092

University of Wisconsin Account #144-T221

for the period of

1 February 1983 to 31 January 1985

submitted by

George Diak
Gary Kirst

Cooperate Institute for Meteorological Satellite Studies
Space Science and Engineering Center
at the University of Wisconsin-Madison
1225 West Dayton Street
Madison, Wisconsin 53706
(608) 262-0544

March, 1986

NATIONAL SCIENCE FOUNDATION
Washington, D.C. 20550

FINAL PROJECT REPORT
NSF FORM 98A

PLEASE READ INSTRUCTIONS ON REVERSE BEFORE COMPLETING

PART I–PROJECT IDENTIFICATION INFORMATION

1. Institution and Address	2. NSF Program	3. NSF Award Number
CIMSS/SSEC University of Wisconsin 1225 West Dayton Street Madison, Wisconsin 53706	Div. of Atmospheric Sci.	ATM 8218092
	4. Award Period From 6/1/83 To 5/31/85	5. Cumulative Award Amount $104,200

6. Project Title
An Investigation of the Utility of High-Resolution Satellite Measured "Skin" Temperatures in Severe Weather Prediction and the Diagnosis of Surface Characteristics

PART II–SUMMARY OF COMPLETED PROJECT *(FOR PUBLIC USE)*

This is a two part study, the aim of which is to improve the treatment of land surface energetics in numerical weather prediction through the use of satellite remote sensing information. In the first part of the study, the sensitivity of numerical forecasts to various surface energy balance parameterizations is examined. It is found that especially precipitation amounts and patterns are quite sensitive to small modulations in this energy balance and problems may exist in specification of surface moisture variables in arid regions. In part two of this study, first results of a land-surface energy budget remote sensing method using soundings from the VISSR Atmospheric Sounder (VAS) are presented. Results are evaluated using forecast model experiments and also through comparisons with an anticedent precipitation index.

PART III–TECHNICAL INFORMATION *(FOR PROGRAM MANAGEMENT USES)*

1. ITEM *(Check appropriate blocks)*	NONE	ATTACHED	PREVIOUSLY FURNISHED	TO BE FURNISHED SEPARATELY TO PROGRAM	
				Check (√)	Approx. Date
a. Abstracts of Theses		X			
b. Publication Citations		X			
c. Data on Scientific Collaborators					
d. Information on Inventions					
e. Technical Description of Project and Results					
f. Other *(specify)*					

2. Principal Investigator/Project Director Name *(Typed)*	3. Principal Investigator/Project Director Signature	4. Date
George R. Diak		

NSF Form 98A (5-78) Supersedes All Previous Editions

Form Approved OMB No. 99R0013

THE INFLUENCE OF VARIATIONS IN SURFACE ENERGY BUDGET PARAMETERIZATIONS ON A SUBSYNOPTIC SCALE MODEL FORECAST

by

STACEY MICHELLE HEIKKINEN

A thesis submitted in partial fulfillment of
the requirements for the degree of

MASTER OF SCIENCE
(Meteorology)

at the

UNIVERSITY OF WISCONSIN - MADISON

1985

ABSTRACT

Surface energy budget parameterizations are shown to significantly influence low level atmospheric variables and precipitation forecast by the CIMSS Subsynoptic Scale Model. Moisture availability is the surface parameter to which the forecast is most sensitive, followed by roughness height and the soil flux parameterization, respectively.

Precipitation and surface temperatures show the most sensitivity to the surface energy budget parameterizations. The sensitivity of atmospheric variables to the surface parameterizations decreases with height and are virtually non-existent above 850 mb.

Comparisons between modeled and VAS measured surface temperatures show that better estimates of surface parameters, in particular soil moisture, will yield more accurate model predicted surface temperatures and consequently will yield a better estimate of the surface energy budget.

The model is able to predict the two most important indicators (frontal position and 500 mb wind direction) of a severe storm associated with upper level northwest flow. The model does poorly in predicting absolute precipitation amounts, but is able to predict the location of the local maxima to within 200 km.

Publications Acknowledging NSF Support
from Grant ATM 8218092

Diak, G.R., S. Heikkinen and J. Bates, 1986: The influence of surface treatment on 24-hour forecasts with a limited area model, including a comparison of modeled and satellite-measured surface temperatures. Mon. Wea. Rev., 114, 215-232.

Diak, G.R., G.A. Mills and G.M. Callan, 1986: The assimilation of satellite data and products into the McIDAS analysis/prognosis/dislay system. Preprint volume Second International Conference on Interactive Information and Processing Systems for Meteorology, Oceanography and Hydrology, Boston, American Meteorological Society, 337-342.

Heikkinen, S.M., 1985: The influence of variations in surface energy budget parameterizations on a subsynoptic scale model forecast. Masters Thesis, University of Wisconsin-Madison, Department of Meteorology, 86 pp.

02/GD/1.1

Table of Contents

ABSTRACT

The effect of variations in surface parameters on 24-hour limited area forecasts have been examined on a day in July 1981. The vehicle for the study is a ten-level primitive equation model covering most of the continental U.S. Variations in moisture availability, surface roughness and soil flux treatment generally do not produce large differences in 24-hour forecasts of primary variables, except in the extreme cases. Precipitation totals, however, are surprisingly sensitive to the surface treatment in several areas where significant amounts of precipitation are evidenced in a control forecast. In these areas, modulations of 10-30% of the control amount due to surface changes are common. In the areas exhibiting principally large-scale precipitation, evidence points to modulations in evaporation as the cause for the precipitation differences. Areas of principally convective precipitation exhibit differences which can be attributed to model-calculated changes in low level moisture convergence patterns between forecasts.

Diurnal surface temperature range measured by the VAS instrument on GOES-3 is compared to those generated in model experiments over the model grid. Good agreement is found in areas with moderate to large moisture availability and roughness heights. Poor agreement is evidenced in the western U.S. where the daytime surface temperature and flux balance is shown to be critically sensitive to small errors in the moisture availability.

First results of a new methodology for estimating the energy budget of the land surface are presented. The method uses the time change of lower atmospheric temperature soundings from the VISSR Atmospheric Sounder (VAS) to estimate surface sensible heating. The method has the potential to

avoid some of the troublesome errors associated with using surface skin temperatures for the same purpose. Results are encouraging in their ability to denote spatial variations in the energy budget.

1. INTRODUCTION

Parameterization of surface energy budget and momentum processes is one of the most difficult tasks in modeling of the planetary boundary layer. While intense in situ investigation can produce realistic values of surface parameters (moisture, momentum and submedium descriptors and albedo) valid at a particular site at a particular time, designating these parameters over the range of surfaces encountered in a global or even a limited area model is a formidable undertaking. Importantly, recent sensitivity studies (Zhang and Anthes 1982, Garrett 1982) using high-resolution PBL models show the sensitivity of boundary layer structure and convective activity to these surface parameters.

Advances are being made on several fronts to deal with the problems of designating surface variables. Comprehensive climatological land cover data sets (Matthews 1983, Kung et al. 1964, Hummel and Reck, 1979) are helpful in estimating their seasonal and geographical distribution, and may be used to infer climatological energy budget and momentum transfer descriptors.

Remote sensing techniques are also offering some insight into parameterization of surface processes and may be useful in assessing shorter term fluctuations in surface variables than can be inferred from the climatological land cover and albedo data bases.

A persistent problem with remote sensing efforts, however, is the lack of adequate verification, since no surface-based research effort to date has produced measurements with sufficient area-coverage to be used as ground-truth for large-area remote sensing methods. Much of the verification must come from less direct indicators.

This research involves remote sensing methods for land surface energy budgets and also surface influences on short term (12-24 hour) forecasts of atmospheric state and precipitation.

As a prelude, some of the surface energy budget and momentum parameterizations in common use in climate and limited-area models were investigated with the intent of providing insight into how surface parameterizations and their variation affect surface temperature, atmospheric structure, and the development of precipitation. Another aim was to acquire some experience as to how common simplifications made in limited-area models (for example, using average rather than area-specific surface parameters) can affect forecast outcome. Of particular interest is the sensitivity of surface temperature to surface variations and comparison of model-generated surface temperatures to their remotely sensed counterparts. All of the methodologies to date which use satellite skin temperature information to diagnose the surface energy balance and/or soil moisture rely on this temperature signal as an indicator of the ratio of sensible to latent heat at the surface.

Finally, we explored a new remote sensing technique using the time change of lower atmospheric temperature from the VAS instrument to denote spatial variations in energy balance, a strategy which essentially uses the atmosphere as a giant calorimeter. There is potential in this methodology to avoid some of the troublesome errors associated with skin temperature methodologies. Prominent among these are the variations in temperature with the surface characteristics or roughness, which for large areas is a very poorly understood conglomeration of smaller surface features within the area.

2. DISCUSSIONS OF RESULTS

2.1 Forecast Sensitivity Experiments

2.1.1 The Forecast Model

The Subsynoptic Scale Model (SSM) is an adaptation of the Australian Region Primitive Equation Model (ARPE) which has been comprehensively documented by McGregor et al. (1978). It has been thoroughly tested in operational conditions with a horizontal resolution of 250 km by the Australian Bureau of Meteorology and in a research mode with a 125 km resolution.

The model in the form used for the U.S. has been amended through the addition of a more comprehensive boundary layer parameterization (to be detailed), the inclusion of Corby differencing (Corby et al. 1972) to better handle the high topographic regions of the continent and the replacement of the original Arakawa-Schubert convective parameterization with a modified Kuo scheme (Kuo 1968, 1974; Hammerstrand 1978). All experiments detailed here were run at a horizontal resolution of 134 Km. Forecast model characteristics are detailed in Table 1.

2.1.2 Boundary Layer Parameterization

Results of the addition of a surface heating scheme to the ARPE have been discussed by Leslie (1980) in experiments investigating the development of the summer heat low over the Australian region. In these experiments, judgments by duty meteorologists indicated superior forecasts in 35 of 37 cases with inclusion of the surface heating scheme.

Our additions to the ARPE PBL formulation include regional assessment of surface parameters (roughness, ground wetness, albedo), addition of stability-dependent transfer coefficients in the surface layer and above, and evaluation of the effects of model-diagnosed clouds on surface

shortwave and longwave radiation. These additions to the SSM parallel independent, but very similar recent additions to the ARPE (G. Mills, personal communication).

2.1.2a Surface and Ekman Layer Treatments

Surface fluxes are calculated via the Monin-Obukhov similarity theory, using the stability functions of Businger et al. (1971) as integrated by Benoit (1976). Above the surface layer the vertical diffusion of heat, momentum, and moisture are parameterized using the Richardson number dependence functions of Blackadar (1979).

2.1.2b Surface Radiation

Shortwave flux at the top of the atmosphere is calculated as a function of geographical location and time of day. Cloud presence and fractional coverage are assessed at three levels as a function of relative humidity (Geylen 1981), and this cloudiness used to calculate the solar flux incident at the surface, using assigned bulk cloud absorption and albedo (Katayama 1972).

Upwelling longwave flux is evaluated using the surface temperature in the Stefan-Boltzmann relationship assuming a surface emissivity of .98, an average for terrestrial surfaces. Downwelling clear air longwave flux is calculated as an empirical function of lowest model level air temperature and humidity (Lettau and Lettau 1978) from the formula

$$LW\downarrow = \sigma T_a^{\,4}(.62 + .0347\sqrt{e_s}) \qquad (1)$$

σ = Stefan-Boltzmann constant ($W\ m^{-2}\ ^\circ K^{-4}$)

T_a = surface air temperature (K)

e_s = surface layer vapor pressure (mb)

This formulation was the most accurate of those tested by Redmond (1980). This clear air flux is augmented for the presence of cloud by a simple methodology outlined in Paltridge and Platt (1976) assuming that the cloud contribution is predominantly in the 8-12 μm atmospheric window region, that the cloud radiative temperature is equivalent to the air temperature at that level and cloud emissivity is unity. No direct shortwave or longwave cooling/heating of the atmosphere is included.

2.1.2c Surface Temperature and Submedium Treatments

Sea surface temperature is held constant through the forecast. Land surface temperature is calculated via a surface energy balance equation

$$S_o(1-A) + LW\downarrow + LW\uparrow + E_o + Q_o + G_o = 0 \qquad (2)$$

S_o = incident surface shortwave flux

$LW\downarrow$ = downwelling longwave flux

$LW\uparrow$ = upwelling longwave flux

E_o = surface evaporative flux

Q_o = surface sensible heat flux

G_o = submedium flux (all $W\text{-}m^{-2}$, sign of fluxes positive towards surface)

A = surface albedo (dimensionless)

Five different methodologies for land surface temperature prediction and determination of the soil flux are available with the SSM. Four of these use instantaneous approximations for the soil flux term of Eq 2 to close the energy balance of the surface. The fifth the "force restore" method (Bhumralkar, 1975) involves a prognostic equation for land surface temperature in which flux exchange between the soil surface layer and deep soil is explicitly considered. The five available methodologies, identical to Bhumralkar (1975) are

1) No soil flux $G_o = 0$

2) $G_o = \lambda/D \cdot (T_s - T_D)$

3) $G_o = C_r \cdot (Rnet)$

4) $G_o = C_q \cdot (Q_o)$

5) $C_1 \, \partial T_g/\partial t = (Rnet+E_o+Q_o) - (\frac{\lambda C\omega}{2})^{\frac{1}{2}} (T_g-\overline{T})$

where λ = soil conductivity ($W\text{-}m^{-2}\text{°}K^{-1}$)

D = damping depth (m)

T_s = soil surface temperature (K)

T_D = soil temperature at depth D

$Rnet$ = net radiation = S_o (1-A) + LW↑ + LW↓

C_r = net radiation constant (dimensionless)

C_q = sensible heat constant (dimensionless)

C = soil heat capacity ($J\text{-}m^{-3}kg^{-1}$)

ω = frequency (sec^{-1})

T_g = surface soil layer temperature (K)

C_1 = $C + (\lambda C/2\omega)^{\frac{1}{2}}$

$\overline{T}$ = deep soil temperature (K)

Soil physical constants for methods two and five are specified as a function of moisture availability similar to Bhumralkar (1975). While there are some differences in specifying these parameters as a function of moisture availability as opposed to ground wetness as defined by Blumralkar (1975), generally differences will not be large (Nappo, 1975), especially considering the general uncertainties in their determination. Subsoil temperature ($\overline{T}$) and soil temperature at damping depth (T_D) are both estimated by using the average surface air temperature for the previous day.

2.1.2d Surface Roughness

The Monin-Obukhov stability functions used to depict transfers in the surface layer require an estimate of the roughness height of the surface.

The roughness height for water surfaces is specified as a function of the lowest model level wind speed through the relationship researched by Garratt (1977).

For land surfaces the roughness height for momentum transfer can be designated as a constant value, as a function of the large-scale topography (Gates and Nelson 1975), or as a function of land use and vegetation character. As suggested by the research of Garratt and Hicks (1973) and Garratt (1978), we may differentiate between the roughness height for momentum transfer vs. those for heat and moisture transfer assuming $Z_{0v} = Z_{0h} = Z_{0m}/\text{constant}$ where Z_0 (h,v,m) are roughness heights for heat, vapor, and momentum transfer respectively. The constant was chosen as 6, an average from the research in these two studies. The climatological distribution of Z_{0m} is shown in Figure 1a.

2.1.2e Surface Evaporation

Land surface evaporation may be controlled through either a moisture availability (MA) or a Bowen ratio. Either of these moisture variables may be designated as a constant over the land area or allowed to vary geographically as a function of a land use and vegetation evaluation. For either option, the value of the surface moisture variable is held constant in time except where significant precipitation occurs, in which case a value appropriate for surface saturation replaces the original.

All forecast sensitivity experiments to be described use moisture availability to depict surface evaporation. In this case of moisture availability, evaporation is parameterized similar to Zhang and Anthes (1982), that is

$$E_o = \rho_a L k_o MA (q_s - q_a)/I_v \quad (3)$$

where

L = latent heat of water ($J\text{-}kg^{-1}$)

ρ_a = dry air density ($kg\text{-}m^{-3}$)

k_o = von Karman constant

MA = moisture availability

q_s = surface saturation specific humidity

q_a = lowest model level specific humidity

I_v = integral Monin-Obukov stability function for vapor transfer

(all dimensionless)

The climatological distribution of moisture availability is shown in Fig. 1b. Later model runs used to verify remote sensing results use a modified moisture parameter appropriate to the remote sensing method, which will be discussed in the relevant section.

Sea surface evaporation is controlled by setting the surface humidity to saturation at the sea surface temperature.

2.1.2f Albedo

Surface albedo can be designated as a constant over the model grid or as a function of researched regional albedo values. These regional values come from Kung et al. (1964). While an albedo determined from satellite techniques (Gautier et al. 1980, Diak and Gautier 1983) was available, this measurement was limited to the spectral band of the GOES satellites ($\sim$.4-.9 μm). Spectral albedo values of both soil and vegetation can change dramatically with wavelength, especially in the near infrared (Norton et al. 1980). It was believed that the total solar albedo measurements from

the Kung et al. research were more appropriate to determine net shortwave than the satellite measurements made in a limited spectral interval.

2.1.3 Sensitivity Experiments; Preliminary - PBL vs. NOPBL Forecasts

All experiments were performed on the day of July 20, 1981. Some attention has been paid to this case (Smith et al. 1982, Peterson et al. 1983) due to the outbreak of severe tornadic storms which occurred at about 20 GMT in central Missouri. A surface analysis at the initial time, 12 GMT, and analyzed 500 mb heights and temperatures are shown in Fig. 2a and b respectively.

At the surface, a cold front extends from Michigan southward to Colorado and drifts slowly southward during the course of the day. At 500 mb cold advection is evident into the upper Great Plains, associated with a jet streak propagating across Wyoming into Nebraska.

Measured precipitation amounts for the 24 hour period beginning 12Z July 20 are shown in Fig. 2c. An area of large scale precipitation in the northeastern and New England states is associated with the eastern Great Lakes low pressure center and leading warm front. Precipitation in the Midwest and Plains is generally associated with convective outbreaks along the twin cold fronts propagating southward during the observation period. Southern Atlantic and Gulf Coast regions experience precipitation which is largely air-mass convective in nature.

A series of 24 hour forecasts were run, beginning at 12 GMT, July 20, 1981, employing various combinations of surface parameterizations as will be described. For comparison purposes it is convenient to describe a "nominal" (NOM) forecast for this time period, employing what we expect to be the best (most rigorous or complete) surface parameterizations available in the SSM. We define this forecast as follows:

1) full time dependent surface and PBL scheme

2) land use and vegetation survey used to designate moisture availability and roughness heights

3) surface temperature and soil flux calculated via force restore method

4) regional measurements used to designate albedo

5) differentiation between roughness heights for momentum vs. heat and vapor, $Z_{0h} = Z_{0v} = Z_{0m/6}$

Several authors have discussed the effects of a PBL parameterization addition to a limited-area model. Our first experiment in general verifies their qualitative results. The addition of surface drag has been noted to limit the intensification of low and high pressure systems (Anthes 1983) as evidenced in sea level pressure. Fig. 3(a-c) shows three 12-hour model forecasts of sea level pressure valid 0 GMT July 21. The first (NOPBL) is one which contains no PBL parameterization at all (no surface fluxes, no vertical diffusion); the second only a time-independent drag coefficient (DRAG) for momentum at the surface (different for land and water); and the third the full time-dependent NOM scheme previously described. Sea level pressure differences over the model grid range from approximately 0-2 mb between the NOPBL and NOM runs. In general, areas of large sensible heating (no clouds, low moisture availability) in the southwest and western states show the largest sea level pressure differences between the two. The differences are greatest after the 12 hour (daytime) period shown and are less-evident in the 24 hour forecast.

Temperature and dewpoint temperature differences for NOM vs. NOPBL experiments are shown at 12 hours in Fig. 4(a-d). Largest areas of temperature difference are in western regions where low values of moisture availability mean considerable sensible heating of the lower atmosphere.

Differences here are also accentuated by the fact that low level (fictitious) values of temperature in high terrain are extrapolated from lowest model sigma level temperatures. In eastern regions the largest temperature differences are in the Ohio Valley and northward in clear portions of the warm sector (e.g., no model diagnosed clouds and resulting high solar forcing).

Low level dewpoint temperatures are higher in most areas in the NOM run, with western states exhibiting the largest increase. Here even a small addition of moisture to the dry air can significantly increase dewpoints. Part of the large increase is also due to the general difficulty in specifying moisture availability in the dry range of values, a topic to be addressed further in section 2.1.8. In the east, as with temperature, the largest dewpoint increases are in the Ohio Valley and northward.

Differences in sea level pressure between the NOPBL and DRAG runs due to inclusion of surface drag are smaller than those reported in other investigations. Both the surface low located over the eastern Great Lakes and the high pressure system in west Colorado show almost no difference between these experiments. Compared to experiments reported by Danard (1969) and Anthes and Keyser (1979), the systems present on July 20 were dynamically weaker and characteristic of a summertime regime. As noted by Anthes (1983), the effect of friction over 24 hours varies from negligible for lighter winds (this case) to extremely important for more vigorous systems. In this case, the role of surface sensible heating appears to be more important on sea level pressure variations than surface frictional effects.

Precipitation amounts over 24 hours between these runs vary, as would be intuitively expected. The NOPBL run shows the least precipitation, with slightly more (.5%) for the DRAG run.

The differences in precipitation for the NOM minus NOPBL runs, however, is substantial at +26% increase of the mean over the domain. Precipitation from the NOM run and differences NOM minus NOPBL are depicted in Fig. 5(a-b). Greatest increases are noted in the major area of large scale precipitation in the northeast states.

In the NOPBL and DRAG runs except for the first several hours (presumably model "spin up" time) precipitation rates are relatively constant over time for the 24-hour forecasts. The addition of the PBL scheme in the NOM run produces a nocturnal maximum in precipitation rate beginning after 0 GMT, principally in this area of large scale precipitation.

The PBL contribution to the nocturnal maximum of storms has long been a studied and modeled phenomenon (Blackadar, 1957). The nocturnal increase in large scale precipitation in the NOM run is due to the development of a large pool of warm, moist air at low levels caused by surface heating and evaporation in clear portions of the warm sector to be south and west (Ohio Valley Area) of model diagnosed clouds. As can be seen in Fig. 4, moist warm air which develops during the day at low levels in these regions in the NOM run will later be advected into the area of the large scale precipitation with an increase in precipitation due to some combination of increased moisture and decreased stability from the low-level warming. Later experiments varying surface parameters (section 2.1.9) will help clarify the roles of latent vs. sensible heating for precipitation amounts.

The beginning of the precipitation increase coincides well with maximum low-level dewpoints and temperatures in the area of large scale precipitation. Although windspeeds at 1000 and 850 mb are quite low in the

NOM experiment, a weak nocturnal maximum does develop southwest of the surface low at about 0600 GMT which may also accentuate precipitation through enhanced moisture and temperature advection at low levels. The nocturnal precipitation increase was also evidenced, in a NOM experiment without the Kuo convective parameterization.

An area of precipitation decrease in NOM vs. NOPBL experiments is evidenced in New York which is a result of a shift in the large-scale precipitation maximum to the southwest. Most areas of strictly convective precipitation exhibit small increases with the addition of the PBL in the NOM run. An exception is an area of significant decrease in an area extending southwest from the Pennsylvania-New Jersey border. Here an examination of model moisture convergence values (the driving force for Kuo precipitation) showed a reduction in NOM vs. NOPBL experiments. Velocity convergence values are not significantly different in this area between these runs and the decrease appears to be caused by a change in low-level wind direction (more cross-isobar flow with the addition of the PBL) and the resulting input of drier air from the east at low levels into the region.

While it is difficult to compare point measurements with model area totals, precipitation patterns from the NOM forecast in general coincide reasonably well with those measured (Fig. 2c) although magnitudes in strictly convective areas appear to be too low. The absolute maximum amount (>3.5 cm) from the forecast is evidenced in central New York State somewhat west of the corresponding measured maximum. The positions of the local smaller measured maxima around North Carolina, Lake Michigan and Arkansas are also depicted in the NOM forecast with about 100 km accuracy. This forecast fails to capture the measured maxima in Wisconsin, Florida and Georgia.

2.1.4 Soil Flux Experiments

Experiments evaluating different surface temperature and soil flux prediction methods have been done by Deardorff (1978) under more controlled conditions, but over a very small area. Our experiments are designed to evaluate performance of these parameterizations over the variety of surface conditions encountered in a limited area model.

The five methods for estimating soil flux outlined previously were evaluated in SSM runs for July 21 to assess their characteristics and assess the sensitivities of forecasts to variations in this surface energy component. Of these methods, 3 and 4 ($G_o = C_q(Q_o)$, $G_o = C_r \cdot (\text{Rnet})$) are highly empirical, basing the soil flux on another component of the surface energy budget. Methods 2 and 5 are simplifications of a fully physical description of the submedium.

Constants employed in the two empirical methods have been researched for both bare soil and vegetation-covered conditions while, strictly speaking, the two physical methods apply only to bare soil. It is common practice at this point in time in many limited area models, however, to employ them over all terrain types with only the roughness height of the surface as a vegetation descriptor, rather than a full canopy model such as Deardorff (1978). The response of all methodologies to this simplification will be of interest.

The magnitude of the soil flux for the four methodologies where this term is not equal to zero (2-5) are shown for one daylight and one nighttime period in the forecasts in Fig. 6. For these forecasts, all characteristics of the NOM experiment have been retained except for varying the soil flux treatment.

The magnitude and direction of the soil flux (positive toward the surface) show noteworthy differences between the four methods investigated.

Of immediate note is the spatial uniformity of the $G_o = C_r \cdot (Rnet)$ (RNET experiment, Fig. 6a-b) at both times. With this method, the main spatial variation in submedium conduction is due to the presence of diagnosed clouds modifying the radiation field. The spatial variation, for example, in the eastern states for the two time periods coincides exactly with cloudy areas. Differences in energy balance components caused by differences in ground wetness and roughness heights over the model grid show little, if any, effect on conduction for this method -- a highly unreasonable condition.

A second undesirable characteristic of the method is evidenced where net radiation becomes small (generally large negative surface-air temperature differences at night). Under these conditions the surface layer may become extremely stable with a cutoff of sensible and latent heat exchange with the atmosphere. The simplified energy budget equation (2) would then be

$$Rnet = G_o \tag{4}$$

and a generalized nighttime constant for soil flux as a function of net radiation ($|C_r| < 1$) is inadequate. Unrealistically low calculated surface temperatures are the result.

The submedium flux predicted by the sensible heat $G_o = C_q \cdot (Q_o)$ (SENS experiment, Fig. 6c-d) shows variations in space which depend heavily on the spatial variation of ground wetness, the chief modulator of the ratio of sensible to latent heat. Variations with roughness height across the model grid are less pronounced since roughness height effects on the sensible/latent heat ratio are secondary to ground wetness. Thus, areas of large sensible heating in the western states during the daytime exhibit the largest soil flux magnitudes. At night these same areas are generally

clear with low winds. The result is low and uniform values of conduction to the surface.

Some spatial variation and higher magnitude are maintained at night in the northeastern U.S. where clouds and somewhat higher winds keep the surface layer from becoming stable enough to damp sensible heating to the surface.

With the SENS experiment, when sensible heat flux approaches zero (nighttime stable conditions), submedium conduction also goes to zero. No energy from the submedium is available to maintain surface temperature and anomalously low calculated temperatures are the result.

Observations have shown that to a good approximation, the amount of energy entering the submedium during daytime hours is returned to the surface at night. While we made no explicit efforts in these forecasts to keep track of the 24-hour net conductive energy to the soil, it can be seen in principle that the SENS method may violate this observation. For example, as shown, clear areas during the daytime are those which conduct the most energy into the submedium, yet those same areas are the ones which tend to be the most stable at night and return the least flux to the surface.

Figs. 7(a-b) show the time trace of conduction flux for a grid point in the Texas Panhandle which was cloud-free and had negligible advective effects (e.g., periodic forcing) for the RNET and SENS experiments. It is clear that neither of these methods approach having the 24-hour net soil flux equal zero.

Both the $G_o = \lambda/D \cdot (T_s - T_D)$ and force restore (KDT and FRES experiments respectively) methodologies for surface temperature determination are simplified physical models of the submedium. Rigorously they apply to bare soil, although it has become common practice to apply them to the "active

surface" (Oke 1978) which, in theory, is a height at which the atmosphere exchanges mass momentum and energy with the surface.

The KDT method relies on the calculated temperature difference between the surface and the sublayer temperature (usually kept constant) to estimate soil flux. A characteristic of this is that the surface temperature, forcing, and soil flux are always in phase, which is disparate with observation of real systems. The FRES method corrects for this deficiency by allowing energy exchange between the surface and deep soil layer. The result is the proper phase relationship of soil flux, forcing, and surface temperature.

The patterns of the magnitude of soil flux for KDT and FRES experiments are generally very similar, as evidenced in Fig. 6(e-h). Relative maxima of conduction exist in western regions with low ground wetness and roughness heights, and minima in the Midwest and East where ground wetness and roughness is greater. An interesting feature of the FRES experiment is the large magnitude of the soil flux compared with all other methods (factors of 1-5) at all the shown observation times. Some of this can be explained by the nature of the method, which for periodic forcing, predicts larger magnitude of soil flux before local noon than after. However, looking at the methods in Fig. 6 (a, c, e, g) at 18 GMT (about local noon in the Midwest), we see that the larger magnitudes relative to other methods persist even in eastern states which are past local noon. The magnitude of the soil flux in the FRES experiment seems unrealistically large for areas of both low and high roughness height (dense and sparse vegetation), compared with observations of these regimes (Oke 1978, Sellers 1965, Garratt and Brost 1981).

By 24 GMT (about 6 pm local time in the Midwest), the soil flux from the FRES method is directed toward the surface over the entire model

domain. This is quite consistent with the observational studies, and the only method which has this characteristic.

Graphically, in Fig. 7c, we see that this property is important in allowing the 24-hour net soil flux to be closest to zero of any of the methods investigated.

For the KDT experiment, magnitudes of soil flux as evidenced in Fig. 6 are much lower than the FRES experiment, and appear more consistent with the aforementioned observational studies over various terrain conditions. The KDT method does not appear to approximate well the condition that 24 hour net soil flux be approximately zero (Fig. 7d).

Both KDT and FRES methods are sensitive to designated roughness height variations, and behave qualitatively correctly to this simple vegetation designation. Fig. 8 (a-b) shows an example at 18 GMT for these two experiments where the roughness heights were lowered to a value appropriate to bare soil. Marked increases in conduction are noted here versus the base experiments in Fig. 6 (e, g). Of note again are the high magnitudes of soil flux predicted by the FRES experiments, which here can be greater than 70% of the net radiation and do not seem reasonable.

The constants used in methods 2 and 5 ($C_{KDT} = \lambda/D$, $C_{FRES} = (\frac{\lambda C\omega}{2})^{\frac{1}{2}}$), applied to the vertical temperature difference to determine soil conduction, may be greatly disparate with one another for the same soil moisture. Fig. 9 shows these two formulations as a function of moisture availability. As shown, the FRES formulation is consistently higher, sometimes by a factor of three, than the equivalent KDT constant. A FRES experiment reducing C_{FRES} by a factor of two yielded more realistic values of soil conduction yet preserved the proper surface temperature-soil flux phase relationship characteristics of the method.

The differences which exist between 24 hour SSM forecasts using the no soil flux condition and the four discussed methods of parameterization of soil flux are small and subtle. While the methods may vary greatly among one another in the amount and timing of the energy exchange with the submedium, large energy differences relative to the soil energy budget are most often small (< 20% of the net shortwave forcing). As a result, there are small differences between these five experiments in the 24-hour forecasts of sea level pressure and primary variables.

Calculated surface temperature spatial patterns are very similar in the FRES, KDT, SENS and RNET experiments except for the previously noted localized nighttime anomalies with the SENS and RNET runs. The extreme differences are in the FRES and NOCOND runs which have the most and least submedium exchange respectively. Daytime differences between the methods average about +3°K for NOCOND vs. FRES. At night, when soil temperature is more sensitive to soil flux variations, the NOCOND temperatures are as much as 10K lower than FRES.

2.1.5 Moisture Availability Experiments

Several experiments were run varying the value of the moisture availability, MA, in an attempt to assess the sensitivity of model forecasts and surface temperature response to this parameter. Forecasts were run, using a distribution of MA from land use and vegetation evaluation (the NOM forecast), the extremes of MA (that is, MA=1 and MA=0) over the entire model grid, and also forecasts setting MA to average values of .2 and .5 over the grid. All other characteristics of the NOM forecast were retained in these experiments.

Differences in primary variables between these forecasts again are not generally large except in extreme cases and are as expected. Highest low

level temperatures and lowest sea level pressures are found for the MA=0 (MA0) experiment which has the most sensible heating of the atmosphere. The MA=1 (MA1) experiment is the opposite extreme, with both the MA=.2 (MA.2) MA=.5 (MA.5) and NOM experiments being close to one another and in the middle of the range for low level temperatures and sea level pressure. Figure 10 shows differences at 12 hours between extreme cases (MA0 minus MA1 experiments) for 1000 and 850 mb temperatures and dewpoints and sea level pressure.

Daytime (18 GMT) sensible and latent heat fluxes in experiments NOM, MA1, MA.5 and MA.2 (Fig. 11 a-g) are not greatly different from one another and are highly non-linear in moisture availability. For MA1 there are several areas where daytime sensible heat flux is directed toward the surface (positive values). The insensitivity of latent heat flux to moisture availability changes in the range of values around .5 has been noted by Nappo (1975). As shown in Fig. 11 even for values in the range around MA=.2 considerable latent heat flux is maintained. Anomalously high evaporation rates due to possible overspecification of moisture availability has been noted by Suarez and Arakawa (1983) and others. Later, in section 2.1.8, a more thorough analysis of the response of surface fluxes to moisture availability will be made.

Large calculated surface temperature differences exist between the extreme MA0 vs. MA1 experiments. During daylight hours surface temperatures in western regions with low roughness heights show as much as +20K difference. Areas with larger roughness heights show typically +10-15K.

At night there is less systematic temperature difference between these experiments evidenced over the entire model grid. In areas where the lower atmosphere is not excessively stable (eastern regions with higher winds,

roughness heights and some clouds), some latent heating is maintained in the MA1 experiment, even at night. The result is lower surface temperatures here than in the MA0 run. In the stable western regions, the increased magnitude of submedium conduction in the MA1 experiment holds surface temperatures somewhat above those in the MA0 run.

2.1.6 Roughness Height Experiments

Several forecasts for July 20 were made, varying the value of the surface roughness over the model grid from the climatological value used in the NOM run. In addition to the climatological distribution, SSM runs were made, using a value of Z_0 = .1 cm, typical of bare soil, and Z_0 = 10 cm, (Z_0.1 and $Z_0$10 experiments respectively).

The differences between forecasts are generally small for sea level pressure and primary variables. Zhang and Anthes (1982) have noted a decrease in latent heating and increase in sensible heating with decreasing roughness height and much of the time this was also observed in our Z_0 experiments. A notable exception to this was in certain low moisture availability areas in the west in the Z_0.1 run. In this case the lowering of Z_0 to .1 had the result of partitioning more energy into the submedium, mostly at the expense of the sensible heat total. Sensible heat fluxes for these areas were lower for the Z_0.1 experiment than either $Z_0$10 or NOM.

In the eastern and midwest states, roughness heights are approximately an order of magnitude larger for the NOM vs. $Z_0$10 experiments. Here, daytime surface temperature differences of about +3K are noted for the $Z_0$10 run. In the western regions the 10 cm value for the $Z_0$10 experiment more closely matches the climatological value in the NOM run, but decreased moisture availability in the area keeps the temperature difference between these experiments about the same as in the East and Midwest. At night

there is very little surface temperature difference between these two experiments.

The Z_0.1 experiment exhibits daytime surface temperatures which are about 6K above the NOM experiment in the East and Midwest and as much as +15K in dry western regions. Once again, at night the Z_0.1 run shows surface temperatures very similar to the other roughness height experiments.

2.1.7 Precipitation Forecasts

As has been discussed in previous sections, the differences between MSLP and primary variables in various soil conduction, moisture availability and roughness height experiments are most often small except for extreme changes. Surprising differences, however, do exist in predicted precipitation amounts between certain of these experiments. In our investigations it became apparent that it would be impossible to explain every difference in precipitation between various experiments. Complicating this precipitation analysis is the interaction of the Kuo convective parameterization with the large scale precipitation formulation in certain areas.

For this reason we ran a second set of experiments duplicating the soil flux, moisture availability and roughness height forecasts but retaining only large scale precipitation. Tables 2 through 4 show large scale precipitation totals over time for these experiments. In the first of this set of experiments (soil conduction sequence) it became apparent to us that precipitation amounts are quite sensitive to even the small surface energy balance modulations caused by changing the submedium parameterization.

In the RNET, SENS, and KDT forecasts, all of which had similar magnitudes of soil conduction (and latent and sensible heating), precipitation

amounts were also very similar to one another (Table 2). The FRES and NOCOND experiments however, with the most and least soil conduction respectively had large-scale precipitation amounts which varied by about +20% FRES vs. NOCOND. The sensitivity of precipitation amount, location and timing was demonstrated in NOM vs. NOPBL experiments (section 3) and these conduction experiments are modulations on that theme. The nocturnal maximum of large scale precipitation noted in section 2.1.3 is clearly shown in these tables.

Subsequent experiments with moisture availability (Table 3) help establish the predominance of latent over sensible heating in this case study for the large scale precipitation amounts. Decreasing soil conduction in previous experiments resulted in both additional latent and sensible heat to the atmosphere and increased precipitation. In the MA experiments increasing moisture availability meant an increase in latent heat, mostly at the expense of the sensible heating total.

Around the area of large scale precipitation in the northeastern U.S. climatological moisture availabilities were about .25 - .35. Precipitation totals for all but the MA0 experiment increase in order of increasing latent heat to the atmosphere, that is MA.2, NOM, MA.5 and MA1, even though the increased latent heat is accompanied by less sensible heating. In these smaller modulations around the climatological MA, precipitation amounts were changed but patterns not greatly modified. The exception to this was the MA0 experiment where surface heating was large enough to create three new areas of large scale precipitation and make the total the largest for any forecast.

Examination of the roughness height experiments (Table 4) yields additional evidence of the importance of process affecting latent heating on precipitation amounts. The increase of latent heating with increased

roughness heights was noted in section 2.1.6. For these experiments again large scale precipitation amounts go in order of increasing latent heating, that is Z0.1, Z010 and NOM.

The addition of the Kuo convective scheme to these experiments makes the precipitation progression much less orderly. In the runs with the Kuo, convective precipitation is responsible on the average for about 75% of the area total. This particular convective parameterization is forced by PBL moisture convergence. In areas of strictly convective precipitation, the modulations of Kuo rainfall amounts almost always could be attributed to different model-predicted moisture convergence values between runs. The most frequent finding in these areas was that moisture convergence and precipitation increased in the experiments in the order of increased sensible heating (the opposite of large scale precipitation). While percentage differences at individual convective locations were usually small compared to the large scale precipitation changes previously discussed, the widespread convective activity on this day made these changes significant in respect to the model total.

2.1.8 Comparison of Modeled and Measured Surface Skin Temperatures

2.1.8a Surface Temperature Measurements

Measured surface temperatures were derived for July 20 from brightness temperature data in two VAS infrared window channels (channel 7 at 12.6 μm and channel 8 at 11 μm), using an empirical algorithm derived by matching VAS clear field of view satellite radiances with reports of sea surface temperature (SST) from NOAA fixed environmental buoys (Bates 1983).

SST's derived from VAS data have undergone extensive evaluation as part of a workshop series sponsored by NASA's Jet Propulsion Laboratory (Njoko 1985). Results from these workshops showed that VAS SST's have a

scatter of .8-1.0 K and a slight warm bias with respect to other remotely sensed and in situ measurements. The two-window channel algorithm was slightly modified over land surfaces to account for higher land surface temperatures and varying land emissivity. Temperature corrections for this two-channel algorithm compared with single window channel temperatures from the GOES satellite correspond well in magnitude with those reported by Zandlo et al. (1982) corrected using TIROS-N water vapor channel measurements.

2.1.8b Temperature Comparisons

Model calculated surface temperatures are sensitive to the initial analysis of lowest level model air temperature. For this reason we place primary emphasis on comparison of diurnal surface temperature range which should be less influenced by initial conditions. It has the added benefit of reducing temperature retrieval errors due to estimation of surface emissivity.

Fig. 12a shows the measured diurnal surface temperature excursion from the VAS instrument, and 12b those calculated from the NOM model experiment previously detailed. Some of the "measured" surface temperatures, mostly in cloudy areas of the eastern third of the U.S., have been interpolated between clear regions where a satellite measurement was possible. As such, they are representative of clear-air surface temperatures. Much of the same area was diagnosed cloudy in the NOM model run and, therefore, the model surface temperatures in these regions are representative of a cloudy regime (reduced insolation), and should not be compared with their interpolated measurement counterparts. Regions of exclusion for temperature comparison are outlined in Figs. 12a and b.

Several observations are immediately apparent in the comparison of the measured and modeled surface temperature range. First, is the relatively good agreement of this range in the east through the midwest. Second is the poor agreement over the western third of the model grid. While measured and modeled surface temperatures in these regions have certain features in common (twin maxima in New Mexico and Wyoming areas, and the general westward increase in surface temperature range), values are systematically lower predicted vs. observed, sometimes by as much as 15K. Nighttime predicted temperatures were quite close to those observed (usually ±3K), and so it is the daytime predicted surface temperatures which are at fault for the large discrepancies.

Suggested causes for these discrepancies between measured and modeled temperatures lies primarily in the climatological assessment of moisture availability used in the model, with the soil flux parameterization (force restore) and assessment of climatological roughness height also being somewhat at fault.

As previously shown, the original force restore soil flux parameterization over-predicts energy into the soil during daytime hours. However, these large errors relative to the soil flux term are generally a small part (10-20%) of the daytime net radiation. As shown in section 5, even in the extreme (NOCOND vs. FRES experiments) the average difference in daytime temperatures due to conduction differences is only about ± 3 K.

Some systematic overestimation of Z_0 in western regions was noted in our survey compared with the more comprehensive analysis of Matthews (1983) which is also a contributing factor to the under-prediction of diurnal temperature range.

Most of the failure of the NOM experiment in duplicating observed surface temperatures, however, comes from the extreme sensitivity of

surface temperatures and the balance of surface fluxes to the moisture availability in the dry range (MA $\leq$ .1). Fig. 13 shows the Bowen Ratio ($B_0 = Q_0/E_0$) plotted at local noon for model grid point with varying values of ground wetness from the NOM experiment. While other differing parameters between grid point (Z_0 and soil flux) can also influence the Bowen Ratio, similar plots for these variables showed ground wetness to be by far the dominating factor.

The sensitivity characteristics of the latent heat flux over the range of MA (Fig. 13) is a result of the expression for evaporation in the methodology (Eq. 3) and its use in a surface energy balance scheme. In large and middle range values of MA, decreasing its value should result in less evaporation, an increase in surface temperature and an increase in the magnitude of other energy sink terms (G_0,Q_0,$LW\uparrow$) in Eq. 2. While this does occur, the decreased evaporation from lowering MA is partially compensated for in Eq. 3 by the increase in saturation vapor pressure at the new higher surface temperature, reducing the potential surface temperature rise and the flux changes. In the drier range of MA however (at higher surface temperatures) the non-linearity of sink terms Q_0 and $LW\uparrow$ in surface temperature means that for a similar decrease in MA there will be less of a surface temperature rise than in the wetter range. Even though the slope of the saturation pressure vapor curve itself is higher at the higher surface temperature, eventually the increase in this e_s term in Eq. 3 with increasing surface temperature does not compensate for decreasing MA, and so the "critical point" in Fig. 13.

This graph points to several unsettling conclusions for the moisture availability as a moisture parameter and its evaluation. Within a range of about 0-.1 surface evaporation is critically dependent on the specification

of MA, and differences as small as several hundredths make large differences in the flux balance and the daytime surface temperature excursion. Outside of this dry range the flux balance is quite insensitive to MA changes.

On the investigation day, July 20, 1981, notable dry anomalies existed in moisture availability in the western states, compared with climatological values. The USDA Crop Moisture Index for this day, with small exceptions, varied from slightly dry to severely dry (vs. climatological) over the model grid west of a line extending from western North Dakota through the Texas Panhandle. Thus, to begin with, the climatological value of MA used in the model is probably an overestimation for this day, and contributes to observed temperature and flux errors.

Even if moisture conditions on this day matched climatological, however, the question remains whether it is possible to initialize MA to the approximately .02 tolerance required to accurately depict surface fluxes in this dry range.

We were able to better approximate the observed maximum of temperature range in the western regions with the aforementioned reduction of force restore soil flux (section 2.1.4), reduction of roughness height and most importantly, reducing moisture availability from .02 to 0.

2.2 Remote Sensing of Surface Energy Budgets Using VAS Soundings

2.2.1 Background - Energy Budget Remote Sensing

Several different techniques have been developed in the last decade for the purpose of remote-sensing of the surface energy budget and/or soil moisture, each with its own characteristics and sources of error.

Microwave techniques (Schmugge, 1980) have the potential to allow direct sensing of the water content of the soil via the effects of water on

soil dielectric properties in the microwave region. Compensation must be made, however, for the presence of foliage above the soil and the change of dielectric properties of the soil with moisture must be known. Translating volumetric soil moisture amounts into a variable for models which accurately depict surface energy balance, especially in the presence of a vegetation canopy, remains a problem.

Several authors have developed techniques for the remote sensing of surface energy budget/soil moisture using the surface temperature information in the thermal infrared portion of the spectrum. The methods have in common that they rely on a signal related to surface temperature indicative of the balance of sensible and latent heat at the surface. When soil moisture information is extracted from this signal, a statistical or physical model of the surface relating soil moisture to the energy balance is required.

The difference between surface and air temperatures in an aerodynamic-energy balance model has been used by Kanemasu (1976) and others to assess evapotranspiration (ET) for cultivated fields. The methodology, however, requires an accurate determination of canopy roughness ($Z_{\emptyset}$) and relies on accurate determination of the small difference between surface and air temperatures. Diak (1980) determined that the technique was feasible for large areas from satellite measurements only for areas of low $Z_{\emptyset}$ and then only to about 2 mm of water (about one-third the range of a typical clear summer-day potential ET). Certain observation condition, notably high wind speeds, cause prohibitive errors.

Price (1982) has demonstrated reasonable results using the 24 hour surface temperature excursion in a simplified model of the earth-atmospheric interface to produce estimates of soil moisture availability and soil thermal inertia. The method relies on an accurate

determination of diurnal sensible heating which over large areas is not well understood, mostly due to uncertainties in surface roughness.

Most recently, Wetzel et al. (1984) have investigated soil moisture retrieval from surface temperature data using as a signal the time change of this temperature in mid morning hours. This parameter was selected on the basis of sensitivity studies using a model of the soil-atmosphere layer. The investigation showed that this time change is also sensitive to $Z_{\emptyset}$, wind speed and biomass which must be accurately taken into account. Other relevant sources of error are noted by the authors. Results showed reasonable correlation with the antecedent precipitation index, a good inference of soil moisture conditions.

Another parameter which has been shown sensitive to the surface sensible/ latent heat balance and soil moisture through our own investigations, investigations by Wetzel et al. (1984), and PBL sensitivity studies such as those of Zhang and Anthes (1982) and Garrett (1982), is the time change in the vertical profile of temperature in the lowest few hundred millibars of atmosphere. This time change in the temperature integral (DTI) which can be expressed as

$$DTI = \Delta\ Cp \int_0^z \rho_a T dz \qquad (5)$$

Cp = heat capacity dry air

ρ_a = air density

T = air temperature

z = vertical coordinate

Δ = time difference

is a direct measure of the gain or loss of heat energy in the air column due to all sources and sinks. For land surfaces, in a clear atmosphere, usually the dominant term among these sources and sinks is the addition of heat energy to the column at the earth's surface. The contributions of notably advection and radiation flux divergence may also be important under certain circumstances.

Under the proper circumstances, evaluation of DTI as an indicator of sensible/latent heat balance has the potential to avoid some of the most troublesome errors involved with using skin temperature information for the same purpose. Important among these error sources is the roughness character of the surface, which for large areas is a poorly-understood conglomeration of smaller roughness features within the area. The time rate of change of surface temperature as well as its absolute value for a given energy balance can change significantly with surface roughness differences. Models for energy balance/soil moisture all of which rely on an explicit or implicit evaluation of sensible heat flux using IR temperatures must deal with the problem of surface roughness and its evaluation. To further complicate matters recent research by Garratt (1973, 1978) indicates that the $Z_{\emptyset}$ for heat transfer may be different than that applicable to the transfer of momentum. Other errors which may be involved in methodologies using IR surface temperatures are those in the temperatures themselves due to emissivity errors or uncertainties in the atmospheric corrections required for the surface temperature determination.

Potentially, DTI is a more direct measure of the sensible heating of the atmosphere than methodologies using IR surface temperatures. The effect of surface roughness is to change the vertical distribution of this energy (Zhang and Anthes, 1982) not the amount, and roughness need not be explicitly considered. Additionally, in models which derive soil moisture

from the energy balance we could expect a better determination of this balance to carry over into a better soil moisture determination.

The potential utility of satellite sounding information in evaluating this DTI and surface flux balance depends both on the information content of the data and our ability to interpret this information. Both these topics will be addressed in subsequent sections.

2.2.2 Potential Use of VAS Information in Remote Sensing of the Surface Energy Balance

The success of the VAS experiment, as proposed by Suomi et al. (1971), has been the result of close collaboration between scientists and engineers from the University of Wisconsin, NASA, NOAA Santa Barbara Research Center and Westinghouse. The first of a series of instruments was put in geostationary orbit aboard the GOES-D satellite (Smith et al., 1981).

The VAS is a radiometer possessing eight visible channel detectors and six thermal detectors which sense atmosphere radiation in twelve spectral bands whose wavelengths lie between 3.9 and 15 μm. The dwell-sound mode of operation of the instrument was designed to enable the interpretation of the vertical temperature and moisture structure of the atmosphere. Channels four, five, six, seven, and nine have vertical weighting functions which peak in the lowest 400 mb of atmosphere and it is largely their information which determines atmospheric retrieval characteristics in the PBL. Typical space and time resolution of these soundings are 50 km and three hours respectively.

Fig. 14(a-f) shows graphically the area of difference (i.e., energy) between VAS retrievals made 6 hours apart (12Z and 18Z) for the case study of July 20, 1981. The different target areas depicted here were all cloud free with negligible low level advection during the six-hour period and

were chosen to represent different climatic regions of surface evaporation of North America.

The six-hour morning period of observation was chosen for the following reasons (similar to Wetzel et al. 1984):

1. To minimize the time for advective and radiative flux divergence effects to develop and accumulate
2. To have a long enough time of solar forcing to insure an adequate signal (temperature change in lower atmosphere)
3. To have a short enough time to not change the time-correlated bias error structure of VAS (to be discussed)
4. Observationally the largest VAS temperature changes in the lower atmosphere occurred within this morning period.

While the exact nature of the information in the soundings may be debated, the difference between moisture regimes is suggested in the differences in areas (DTI) between these sets of soundings. This information encouraged us in seeking means to quantify this signal.

As a first step in this effort, a quantitative evaluation of the heat energy difference (DTI) for the same six hour period was made from VAS soundings pairs for all portions of the continental U.S. For each sounding pair the evaluation was made from the surface up to a level 400 mb above the surface. While this is a deeper layer than is normally thought of as the PBL, it was chosen to take into account the broad vertical weighting functions (i.e. coarse vertical resolution) of VAS and tendency to average temperature features in the vertical.

Since the area coverage was so extensive and the amount of solar forcing varied noticeably in the six hour period over the domain, it was desirable to normalize the results of the DTI calculations by some measure of input or available energy. The net radiation total over the same six

hours was the logical first choice due to its implications for available energy at the surface. In clear air it can be well-approximated from satellite information (Diak, 1980).

Advective effects at lower atmospheric levels (although not very significant for this case in the 12Z-18Z investigation period) were compensated for by using the SSM, run without diabatic surface and PBL processes for the time period, to estimate an approximate advective temperature correction at model levels in the lowest 400 mb. Radiative flux divergence effects were also evaluated through the use of VAS radiances (Smith and Woolf, 1983) and were found to be negligible.

Figure 15 shows the results of this calculation over the North American survey region. This figure depicts the geographical representation of calculated DTI (corrected for advection) normalized (NDTI) by the estimated net radiation. Areas of probable cloud contamination are contoured in dashed lines. Although absolute percentages are quite realistic the figure at this point is best viewed in terms of relative results between geographical regions and moisture regimes. Figure 16 shows for comparison purposes the moisture supply of the U.S. (after RabenHorst, 1981). The VAS results in this early stage of development appear very reasonable in depicting spatial differences in energy budget climatology.

2.2.3 Interpretation of Results

Observational confirmation of surface fluxes over the spatial scales involved in this study are unfortunately totally nonexistent and we must rely on less direct indicators of the validity of results.

Visual comparison of NDTI results to climatological moisture information (Figs. 15 and 16) was quite encouraging. Absolute magnitudes of NDTI values are reasonable in wet and dry regions and the tight horizontal gradient through the Great Plains is well-depicted. For these reasons, it was decided initially to use the NDTI values unmodified to perform several indirect verification experiments which will be described.

2.2.3a Comparison of NDTI with Anticedent Precipitation Index

The anticedent precipitation index (API) is considered the best ground truth linear approximation to area average soil moisture available on a routine basis over large areas (Blanchard et al. 1981, Wetzel et al. 1984). The API for day i is calculated from the expression

$$API_i = P24_i + K(API_{i-1}) \qquad (6)$$

P24 is the 24-hour precipitation total on day i and K is a depletion constant which depends on area and season.

API values were computed for July 20, 1981 for the continental United States using 24 hour totals of precipitation from the SVCA network for the prior 30 days. Results at the SVCA location were then objectively analyzed to a uniform grid. Results of this procedure are shown in Fig. 17. Visually, there is a good correspondence between this calculated API and the NDTI values in Fig. 15. To compare these more quantitatively it was desirably to make a transformation of the API to an index which represents evaporation at the surface (related through energy budget considerations to NDTI) which is generally non-linear in soil moisture (e.g. API).

To do this, we use a model developed by Wetzel et al. (1984) which relates surface evaporation to root zone soil moisture. While the modeled evaporation depends on a number of local environmental constants, the general relationship is of the form

$$E_0 \alpha \sqrt{W} \quad \alpha \quad \sqrt{API} \tag{7}$$

W = root zone soild moisture (in)

Statistical evaluation of NDTI versus $\sqrt{API}$ over the areas of the continental U.S. which were cloud free for the observing period yielded a correlation coefficient of between .6 and .7 depending on the degree of smoothing used to objectively analyze the API results to a gridded field. For these analysis purposes, a recursive filter was used (Holl, 1967) to produce API grids at various smoothings. This recursive filter has a very sharp wavelength cutoff which can be adjusted to eliminate features below a specified spatial scale. The best correlation (.7) was obtained at a cut-off wavelength of 300 km, suggesting that the NDTI information may be most useful at this spatial interval. Including some of the regional constants which rigorously apply in Eq. 7 may improve the correlation.

Indications from the NDTI versus API comparison are that the NDTI values may need some additional calibration in arid areas. There are several large areas in western states where the API is essentially zero (Fig. 17). Diagnostic relationships between API and soil moisture indicate that soil moisture should be well below the wilting point for these regions (most of the net radiation going into sensible rather than latent heat) and thus the NDTI values for these regions are probably somewhat low.

2.2.3b Forecast Model Comparisons

An examination of the impact of using NDTI information on numerical for the case study day of July 20. To do this, NDTI values were transformed into a simple surface moisture index which we will term flux evaporivity (FE) where

$$FE \equiv (E_0/Rnet) = 1 - NDTI - (G_0/Rnet) \tag{8}$$

While it is possible to calculate a number of moisture parameters from the NDTI information, for this first test the FE was chosen because of its simplicity and straightforward calculation from the satellite information.

This diagnostic FE relationship requires that the soil flux G_0 be specified. A number of soil flux parameterizations were examined in section 2.1.2 of this report for prognostic purposes; however, the choice for this diagnostic purpose is not as sensitive. Errors in soil flux, generally a small term in the energy balance equation will translate the small errors in the caluclation of FE.

Statistical relationships similar to those described in section 2.1.2, basing the soil flux on sensible heating, net radiation or other variables were evaluated for a range of environmental conditions using a research quality version (explicit subsoil layers) of the PBL model previously described. The strongest statistical correlation was found in a previously unexplored relationship between the fraction of the net radiation going into conduction (G_0/Rnet) and the logarithm of the roughness height, (G_0/Rnet) increasing with decreasing roughness height Z_o and a correlation coefficient of .95. Conceptually, it can be seen that increasing Z_0 increases the effectiveness of turbulent transport of energy away from the surface with a resulting decrease in surface temperature and conduction energy. This relationship was used to diagnose the quantity (G_0/Rnet) in Eq. 8. The resultant field of FE values for the continental United States is shown in Fig. 18.

A duplicate of the modified NOM forecast previously detailed (reduced Z_0 and modified conduction constants) was made using the FE to control daytime surface evaporation instead of moisture availability. Land surface evaporation was then described in the model by the relationship

$$E_0 = - FE \cdot Rnet \qquad (9)$$

for daytime conditions.

For evaluation of the results of this experiment we examined the 12-hour change of lower level model air temperature between these two model runs using analyses from RAOB data at as verification. Comparisons were made on the two lowest model sigma surfaces (τ = .998, 898) rather than on pressure surfaces to reduce potential temperature extrapolation errors to standard pressure surfaces in regions of high topography.

Standard errors in temperature over the continental U.S. were reduced at these two levels by 19% and 4%, respectively, in the FE versus modified-NOM experiments. Most of the improvements came in western states where problems with over-specification of moisture availability have been extensively discussed. S1 skill scores for these two low level temperatures were also decreased by about four points.

Model-calculated diurnal surface temperature range from the FE experiment are shown in Fig. 19 and may be compared to satellite measurements and prior modeling work in Fig. 12. Distinct improvements are noted in the FE experiment versus satellite measurements in the sharpening of the east-west gradient through the Great Plains and in the position of the maxima. While absolute values show marked improvements, they are still somewhat low compared with the satellite measurements, supporting some prior indirect evidence from the API comparison that NDTI and resulting FE calculations may need some additional calibration in these regions to lessen the amount of energy going into latent heating.

2.2.3c Error Discussion

There is little knowledge available on the absolute accuracy of VAS land surface sounding products chiefly due to the lack of surface

observations at a comparable space and time scale to use as verificaton. For these methodologies, which rely on a time difference calculation it is not necessary that absolute values of radiances or derived temperatures be correct, only that time differences be well-depicted. Bias errors which are constant over the observation period will not affect calculations.

Jedlovec (1984) has done an error analysis of VAS retrievals using high density space and time RAOB soundings produced during the AVE/VAS experiment of March 6, 1982 over the central U.S. In this case, for our chosen six hour morning observation period bias errors were relatively constant in time for the physical retrieval methods which are used at SSEC. While it is hard to generalize from one study, this March 6 day represents a "worst case scenario" for VAS retrievals in the PBL, with the presence of a strong and fast-moving frontal inversion (known to affect retrieval error) in the region of study, and one we would avoid in practice. Further research is needed to investigate the error structure of VAS information and products with what information exists.

The vertical broadening of averaging of temperature features in the vertical in VAS retrievals due to the broad vertical weighting functions of the various channels is a well-known characteristic of the retrieval system. This may not necessarily be a fault for these purposes (and may even be an asset) since we are interested in average changes over a layer at least several hundred millibars deep.

In looking for a surface energy balance signal to lower atmosphere temperature change it has been assumed that other effects (advection, radiative flux divergence) are either negligible or can be approximately corrected for. Obviously, this is not always true. Temperature advection has been taken into account in an approximate manner for the results shown

in Fig. 18, but under highly advective circumstances (fast moving fronts) or circumstances unresolved by the forecast model (sea breeze, slope winds, etc.) we cannot expect to do as well. Similarly, circumstances can be envisioned, however, for example in the presence of sharp vertical temperature or moisture gradients where radiative flux divergence is large and uncertain.

It is not necessary to apply methods developed at all places at all times. The knowledge of methodology errors which is gained in developing correction estimates for advection and flux divergence should enable the correct spatial and temporal choices for observation periods, to develop an optimal sampling strategy.

From this preliminary investigation it appears that there is information content in the data, but it is probable that derived sounding products, while convenient, do not constitute their most effective use. VAS temperature retrievals are subject to errors which are not yet well-understood and are dependent on the characteristics of the particular retrieval algorithm used to go from radiance to temperature. A likely alternative is that the VAS radiances in channels describing PBL levels may be more effective in describing surface energy balance than the soundings themselves and further research sould be directed at this possibility.

2.3 Conclusions and Recommendations

The sensitivity of numerical forecasts to variations in moisture availability, roughness length and soil flux has been documented in a case study for summer 1981. Generally, differences in forecasts of primary variables are not large except in extreme cases. Modulations in large scale precipitation amounts however were significant even for small differ-

ences in surface energy balance. In an extreme experiment, setting surface moisture availability to zero, surface heating was large enough to create several areas of large scale precipitation not evidenced in the control run. Areas of convective precipitation were also affected by surface energy balance modulations.

Implications are that boundary layer and precipitation (convection) parameterizations must be developed and tuned in unison for precipitation prediction and that an accurate local representation of the surface will be required. Model sensitivity to surface variations also suggests that anomalies in surface properties from climatological values may be important in certain synoptically sensitive areas, and thus remote sensing of surface energy budgets may have a role in short term forecasting.

Of the soil flux methods examined, two, the RNET and SENS methods, are undesirable because of anomalous surface temperatures at night, poor response to surface roughness characteristics, and poor 24-hour flux conservation, which may have an impact in longer term (climate) forecasts. The KDT method also does not predict 24-hour net flux well, but does well for instantaneous flux magnitude. The FRES method well conserves the 24-hour flux but over-predicts instantaneous values. Lowering the constants associated with conduction in the FRES method may well alleviate some of its over prediction.

Surface temperatures and temperature range were relatively well-predicted in areas with moderate to high roughness heights and ground wetnesses and are not very sensitive in those regions to errors in these parameters. However, in dry regions with low roughness heights, small errors in the assessment of moisture availability (a moisture parameter in very common use in climate and limited-area models) cause very large errors

in surface temperature and the surface flux balance. This suggests that a very careful climatological evaluation of moisture availability need be made, or that an alternative moisture variable be chosen for which small errors do not have such drastic effects. Remote sensing of the surface energy balance to calibrate moisture variables with diagnosed surface fluxes may also help alleviate problems with specification of surface moisture variables.

A new method of remote sensing of the surface energy budget through use of VAS temperature soundings has the potential to circumvent some of the problems with other thermal infrared methodologies developed for the same purpose and is suitable to surveying the large areas involved in weather and climate modeling. First results of this procedure yielded reasonable spatial variations in surface evaporation and results correlated well with a calculated anticedent precipitation index. A limited-area model forecast of PBL temperatures was improved using the satellite-derived surface evaporation description versus one which used a climatic moisture availability. Further calibration of the methodology and extraction of the best "signal" (most probably VAS radiances instead of temperatures) is necessary to make the technique most useful.

02/GD/01

REFERENCES

Anthes, R.A., 1983: Regional models of the atmosphere in middle latitude. Mon. Wea. Rev., 111, 1306-1355.

_____ and D. Keyser, 1979: Tests of a fine mesh model over Europe and the United States. Mon. Wea. Rev., 110, 1187-1213.

Bates, J.J., 1983: Satellite-derived sea surface temperature: Workshop I. JPL Publication 83-34. Jet Propulsion Laboratory, California Inst. of Technology, Pasadena, CA 91109.

Benoit, R., 1976: A Comprehensive Parameterization of the Atmospheric Boundary Layer for General Circulation Models, NCAR Cooperative Thesis No. 39, National Center for Atmospheric Research, Box 3000, Boulder, CO 80307, 278 pp.

Bhumralkar, C.M., 1975: Numerical experiments on the computation of ground surface temperature in an atmospheric circulation model. J. Appl. Meteor., 14, 1246-1258.

Blackadar, A.K., 1957: Boundary layer wind maxima and their significance for the growth of nocturnal inversion. Bull. Am. Meteor. Soc., 38, 283-290.

_____, 1977: High resolution models of the planetary boundary layer. Advances in Environmental Science and Engineering, Vol. 1. Gordon and Breach, 50-85.

Blanchard, B.J., M.J. McFarland, T.J. Schmugge and E. Rhoades, 1981: Estimations of soil moisture with API algorithms and microwave emission. Water Res. Bull., 17, 767-774.

Businger, J.A., J.G. Wyngaard, Y. Izumi, and E.F. Bradley, 1971: Flux profile relationships in the atmospheric surface layer. J. Atmos. Sci., 28, 181-189.

Corby, G.A., A. Gilchrist, and R.L. Newson, 1972: A general circulation model of the atmosphere suitable for long period integrations. Quart. J. Roy. Meteor. Soc., 98, 809-832.

Danard, M.B., 1969: Numerical effects of surface friction on large scale atmospheric motions. Mon. Wea. Rev., 97, 835-844.

Deardorff, J.W., 1978: Efficient prediction of ground surface temperature and moisture with inclusion of a layer of vegetation. J. Geophys. Res., 83, 1889-1903.

Diak, G.R., 1980: The utility of satellite data in estimating the energy budget of the earth's surface. Ph.D. Thesis, Department of Meteorology, University of Wisconsin-Madison, 99 pp.

_____, and C. Gautier, 1983: Improvements to a simple physical model for estimating insolation from GOES data. J. Appl. Meteor., 22, 505-508.

Gadd, A.J., and J.F. Keers, 1970: Surface exchange of sensible and latent heat in a 10-level model atmosphere. Quart. J. Roy. Meteor. Soc., 96, 297-308.

Garratt, J.R., and B.B. Hicks, 1973: Momentum, heat, and water vapour transfer to and from natural surfaces. Quart. J. Roy. Meteor. Soc., 99, 680-687.

_____, 1977: Review of drag coefficients over oceans and continents. Mon. Wea. Rev., 105, 915-928.

_____, 1978: Transfer characteristics for a heterogeneous surface of large aerodynamic roughness. Quart. J. Roy. Meteor. Soc., 104, 491-502.

_____, and R.A. Brost, 1981: Radiative cooling effects within and above the nocturnal boundary layer. J. Atm. Sci., 38, 2730-2746.

Garrett, A.J., 1982: A parameter study of interactions between convective clouds, the convective boundary layer, and a forested surface. Mon. Wea. Rev., 110, 1041-1059.

Gates, W.L., and A.B. Nelson, 1975: A new (revised) tabulation of the Scripps topography on a 1° global grid. Part I: Terrain heights. Rep. R-1276-1-ARPA. The Rand Corporation, 1700 Main St., Santa Monica, CA 90406, 132 pp.

Gautier, C., G. Diak, and S. Masse, 1980: A simple physical model to estimate solar radiation at the surface from GOES satellite data. J. Appl. Meteor., 29, 1005-1012.

Geylen, J.F., 1981: Some diagnostics of the cloud/radiation interaction in the ECMWF forecasting model. Workshop on Radiation and Cloud Interaction in Numerical Modelling, Shinfield Park, United Kingdom, 15-17 October 1980. European Center for Medium Range Weather Forecasting, Shinfield Park, U.K., 209 pp.

Holl, M.M., 1967: A new version of the beta program for an 89x89 grid. Technical Note No. 1, Contract NOO228-67-C-2759. Meteorology International, Inc., Monterey, California.

Hammerstrand, U., 1977: On parameterization of convection for large scale numerical forecasts at mid latitudes. Beiträge zur Physik der Atmosphäre, 50, 78-88.

Hummel, John R., and R.A. Reck, 1979: A global surface albedo model. J. Appl. Meteor., 18, 239-253.

Jedlovec, G.J., 1984: A statistical evaluation and comparison of VISSR Atmospheric Sounder (VAS) data and corresponding rawinsonde measurements. NASA Technical Memorandum 82575, 11 pp.

Kanemasu, E.T., L.R. Stone and W.L. Powers, 1976: Evapotranspiration model tested for soybean and sorgum. Agron. J., 68, 569-572.

Kasahara, A., and W. Washington, 1971: General circulation experiments with a six-layer NCAR model, including oragraphy, cloudiness, and surface temperature calculations. J. Atmos. Sci., 28, 657-701.

Katayama, A., 1972: A simplified scheme for computing radiative transfer in the troposphere, Technical Report No. 6, Department of Meteorology, University of California at Los Angeles, 405 Hilgard Avenue, Los Angeles, CA 90024, 77 pp.

Kung, E.C., R. Bryson, and D. Lenschow, 1964: Study of a continental surface albedo made on the basis of flight measurements and structure of the earth's surface cover over North America. Mon. Wea. Rev., 92, 543-564.

Kuo, H.L., 1964: On formation and intensification of tropical cyclones through latent heat release by cumulus convection. J. Atmos. Sci, 22, 40-63.

_____, 1974: Further studies of the parameterization of the interaction of cumulus convection on large-scale flow. J. Atmos. Sci., 31, 1232-1240.

Leslie, L.M., 1980: Numerical modeling of the summer heat low over Australia. J. Appl. Meteor., 19, 381-387.

Matthews, 1984: Prescription of land-surface boundary conditions in GISS GCM 11: A simple method based on high-resolution vegetation data bases. NASA Technical Memorandum 86096, Goddard Space Flight Center, New York, New York, 10025, 20 pp.

McGregor, J.L., L.M. Leslie, and D.J. Gauntlett, 1978: The ANMRC limited area model: consolidated formulation and operational results. Mon. Wea. Rev., 106, 427-438.

Nappo, C.J., 1975: Parameterization of surface moisture and evaporation rate in a planetary boundary layer model. J. Appl. Meteor., 14, 289-296.

Njoko, E.G., 1985: Satellite-derived sea surface temperature: workshop comparisons. Bull. Amer. Meteor. Soc., 66, 274-281.

Norton, C., F. Mosher, B. Hinton, D. Martin, D. Santek, and M. Kuhlow, 1980: A model for calculating atmospheric turbidity over the oceans from geostationary satellite data. J. Appl. Meteor., 19, 633-644.

Oke, T.R., 1978: Boundary Layer Climates, John Wiley & Sons, 372 pp.

Paltridge, G.W., and C.M.R. Platt, 1976: Radiative Processes in Meteorology and Climatology. Elsevier Scientific Publishing Company, 318 pp.

Peterson, R.A., D. Keyser, A. Mostek, and L. Ucellini, 1983: Severe storms analysis and forecasting techniques using VAS satellite data. Proceedings 13th Conf. Severe Local Storms, Boston, Amer. Meteor. Soc., 375 pp.

Price, J.C., 1982: On the use of satellite data to infer surface fluxes at meteorological scales. J. Appl. Meteor., 21, 1111-1122.

RabenHorst, T.D., 1981: Climate and agriculture: An atlas of the United States. Dept. of Geography, University of Maryland, 83 pp.

Redmond, K., 1980: An emissivity parameterization suitable for climate modeling. J. Appl. Meteor., 108, 663-675.

Schmugge, T.J., T.J. Jackson and H.L. McKim, 1980: Survey of methods for soil moisture determination. Water Resour. Res., 16, 961-979.

Sellers, W.D., 1965: Physical Climatology. University of Chicago Press, 272 pp.

Smith, W.L., V.E. Suomi, W.P. Menzel, H.M. Woolf, L.A. Sromovsky, H.E. Revercomb, C.M. Hayden, D.. Erickson, and F.R. Mosher, 1981: First sounding results from VAS-D. Bull. Amer. Meteor. Soc., 62, 232-236.

_____, V.E. Suomi, F.X. Zhong, and W.P. Menzel, 1982: Nowcasting applications of geostationary satellite atmospheric sounding data. Nowcasting, Academic Press, 123-135.

_____, and H.M. Woolf, 1983: Geostationary satellite sounder (VAS) observations of longwave radiation flux. Paper presented at Igls Conference on Satellite systems to measure radiation budget parameters and climate change signals, Austria, Aug. 29-Sept. 2.

Suarez, M.J., A. Arakawa and D. Randall, 1983: The parameterization of the planetary boundary layer in the UCLA general circulation model: formulation and results. Mon. Wea. Rev., 111, 2224-2243.

Suomi, V.E., T. VonderHaar, R. Krauss and A. Stamm, 1971: Possibilities for soundings the atmosphere from geosynchronous spacecraft. Space Research XI, pp. 609-617.

Zandlo, J.A., W.L. Smith, W.P. Menzel, and C.M. Hayden, 1982: Surface temperature determination from an amalgamation of GOES and TIROS-N radiance measurements. J. Appl. Meteor., 21, 44-50.

Zhang, D., and R.A. Anthes, 1982: A high resolution model of the planetary boundary layer-sensitivity tests and comparisons with SESAME-79 data. J. Appl. Meteor., 21, 1595-1609.

LIST OF ILLUSTRATIONS

Figures

Figure 11 18 GMT forecasts of sensible and latent heat for NOM (a-b), MA1(c-d), MA.5 (e-f) and MA.2 (g-h) experiments. All $W\text{-}m^{-2}$.

Figure 12 Diurnal surface temperature excursion (K) measured from VAS (a) and modelled in NOM experiment (b).

Figure 13 Bowen ratio vs. ground wetness (both dimensionless) at local noon calculated from NOM experiment.

Figure 14 Difference in VAS retrievals made six hours apart for different moisture regions of the continental United States on July 20, 1981.

Figure 15 Dimensionless ratio (NDTI) of sounding energy to net radiation for the cloud free areas of the continental United State, July 20, 1981 (% x 100).

Figure 16 Climatic moisture regions of the United States (after RabenHorst, 1981).

Figure 17 Anticedent precipitation index (in x 100) for the continental United States, July 20, 1981.

Figure 18 Flux evaporivity (% x 1000) for cloud-free areas of the continental United States, July 20, 1981.

Figure 19 Diurnal surface temperature range (K) from IFE model experiment, July 20, 1981.

Tables

1. Forecast model characteristics.

2. Large-scale precipitation per area vs. time for soil conduction experiments. Arbitrary units.

3. Same as table 2, but for ground wetness experiments.

4. Same as table 2, but for roughness length experiments.

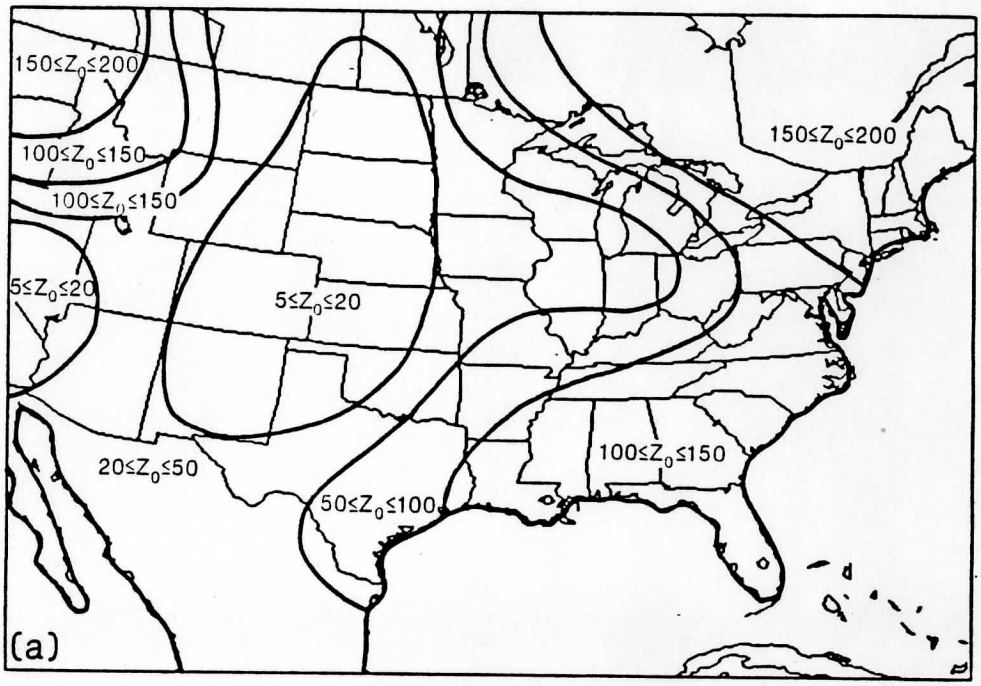
150≤Z0≤200
100≤Z0≤150
100≤Z0≤150
5≤Z0≤20
5≤Z0≤20
150≤Z0≤200
20≤Z0≤50
50≤Z0≤100
100≤Z0≤150
(a)

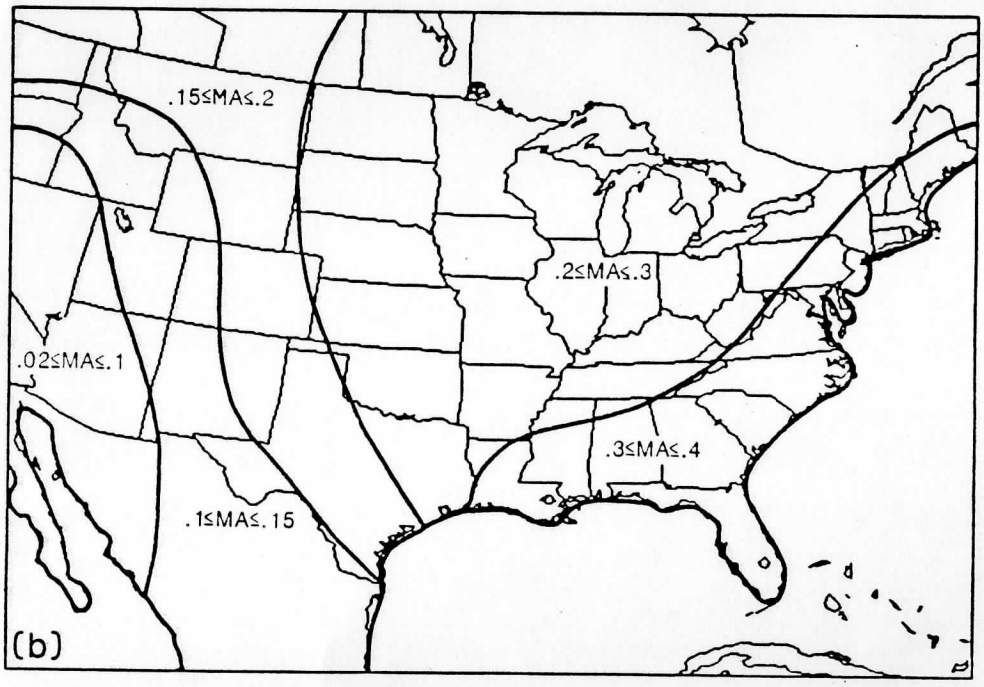
.15≤MA≤.2
.2≤MA≤.3
.02≤MA≤.1
.3≤MA≤.4
.1≤MA≤.15
(b)

FIG 1

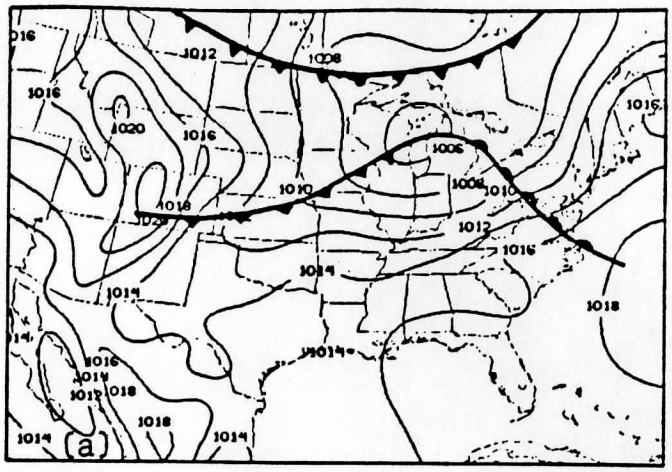
1012
1008
1016
1020
1016
1010
1008
1010
1012
1016
1014
1014
1018
1016
1014
1012
1018
1018
1014
1014
(a)

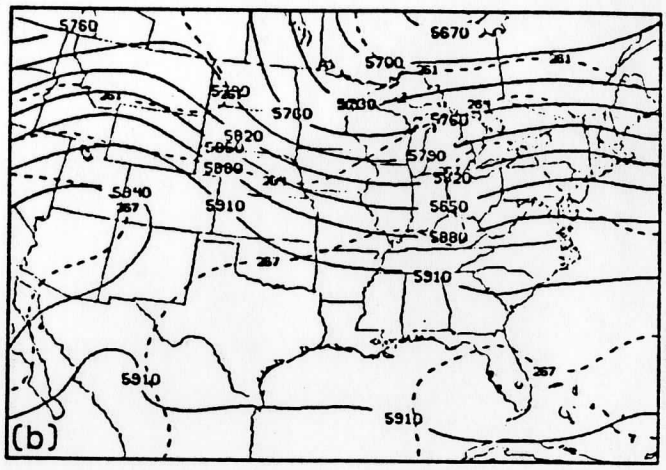
5760
5670
5700
5700
5760
5820
5790
5880
5840
5910
5650
5880
5910
5910
5910
(b)

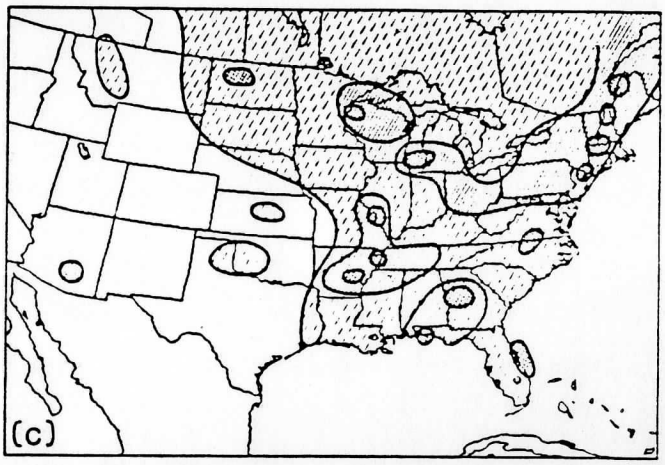
(c)

FIG 2

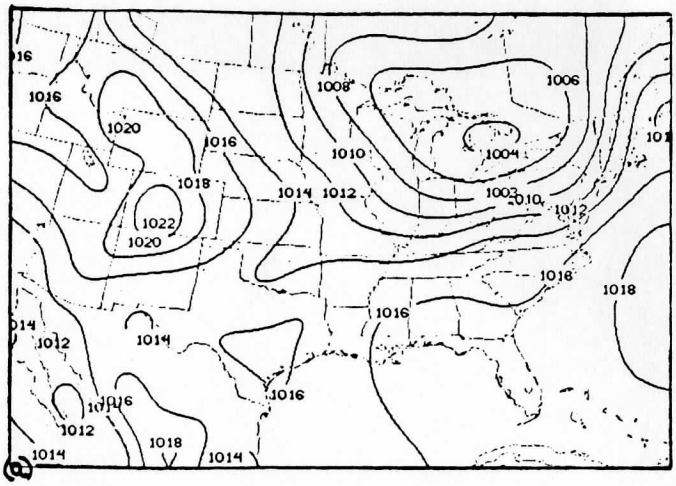
(a)
1016
1008
1006
1016
1020
1016
1010
1004
1018
1014
1012
1003
1010
1012
1022
1020
1018
1018
1016
1014
1012
1014
1016
1016
1012
1018
1014
1014

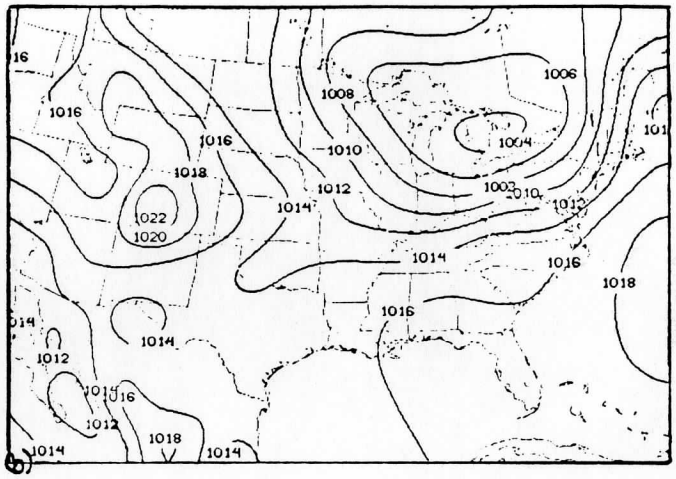
(b)
1016
1008
1006
1016
1016
1010
1004
1018
1012
1003
1010
1014
1012
1022
1020
1014
1016
1018
1016
1014
1012
1016
1016
1012
1018
1014
1014

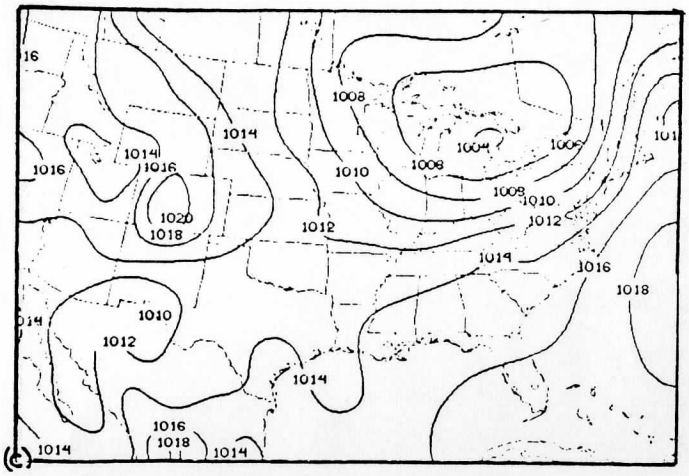
(c)
1016
1008
1014
1004
1006
1014
1016
1016
1010
1008
1008
1010
1020
1018
1012
1012
1014
1016
1018
1010
1012
1014
1016
1018
1014
1014

FIG 3

FIG 4

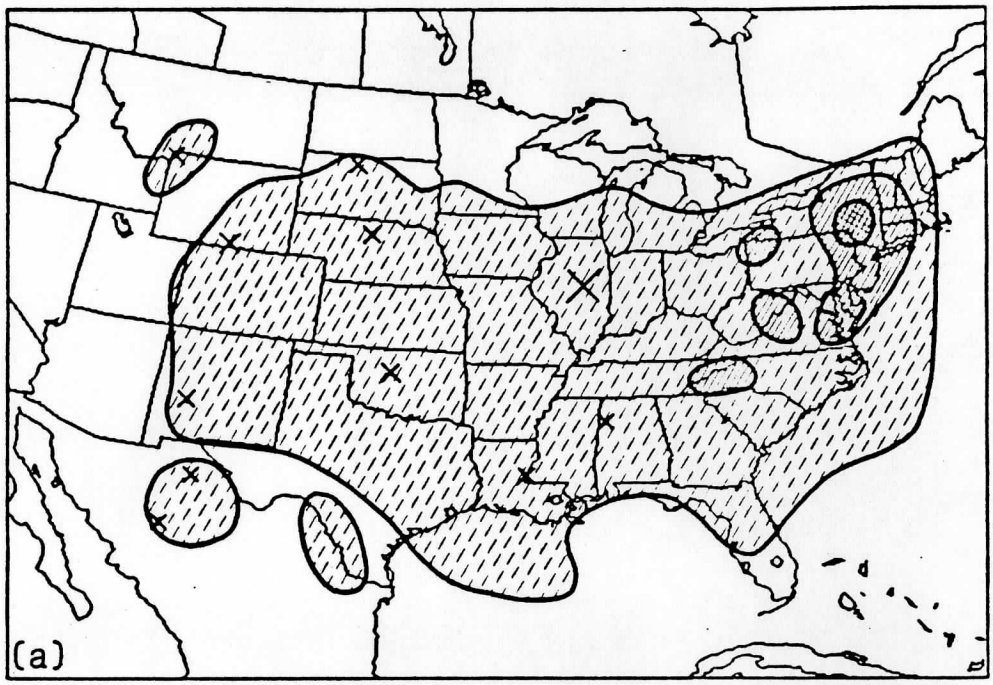

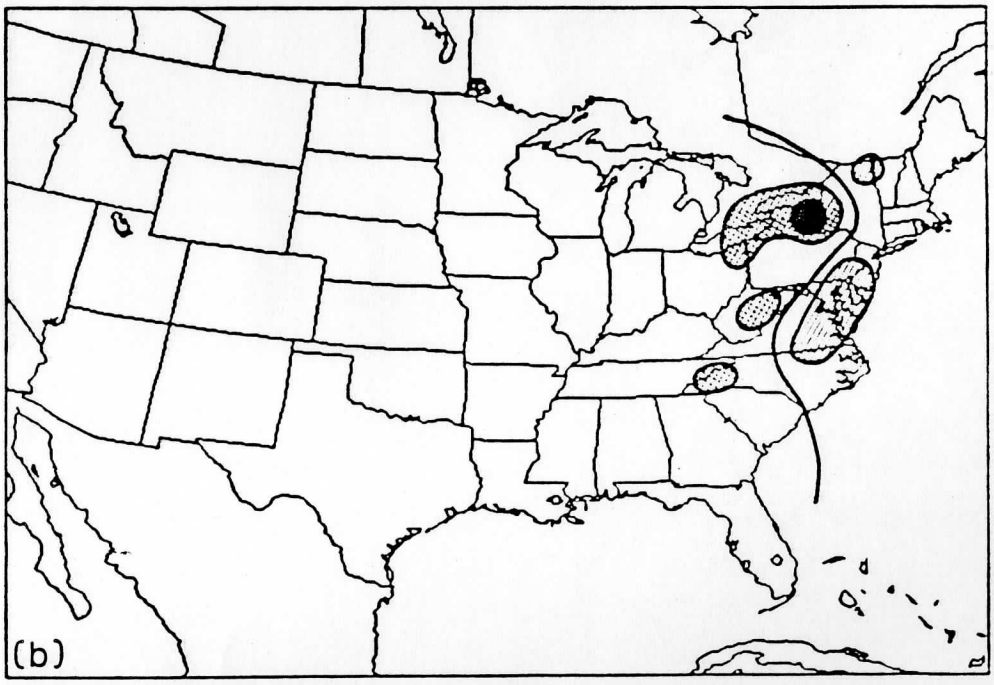

FIG 5

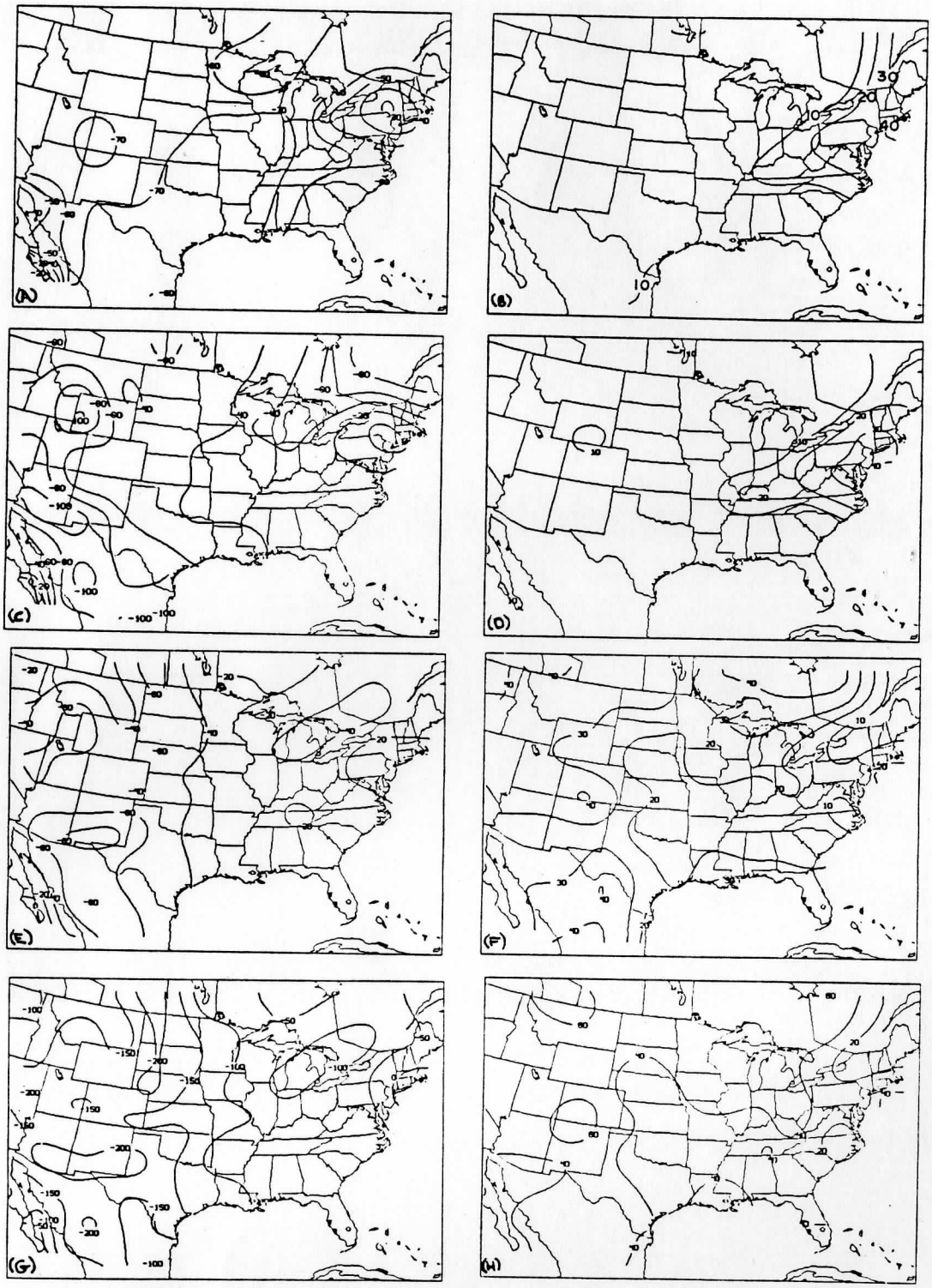

FIG 6

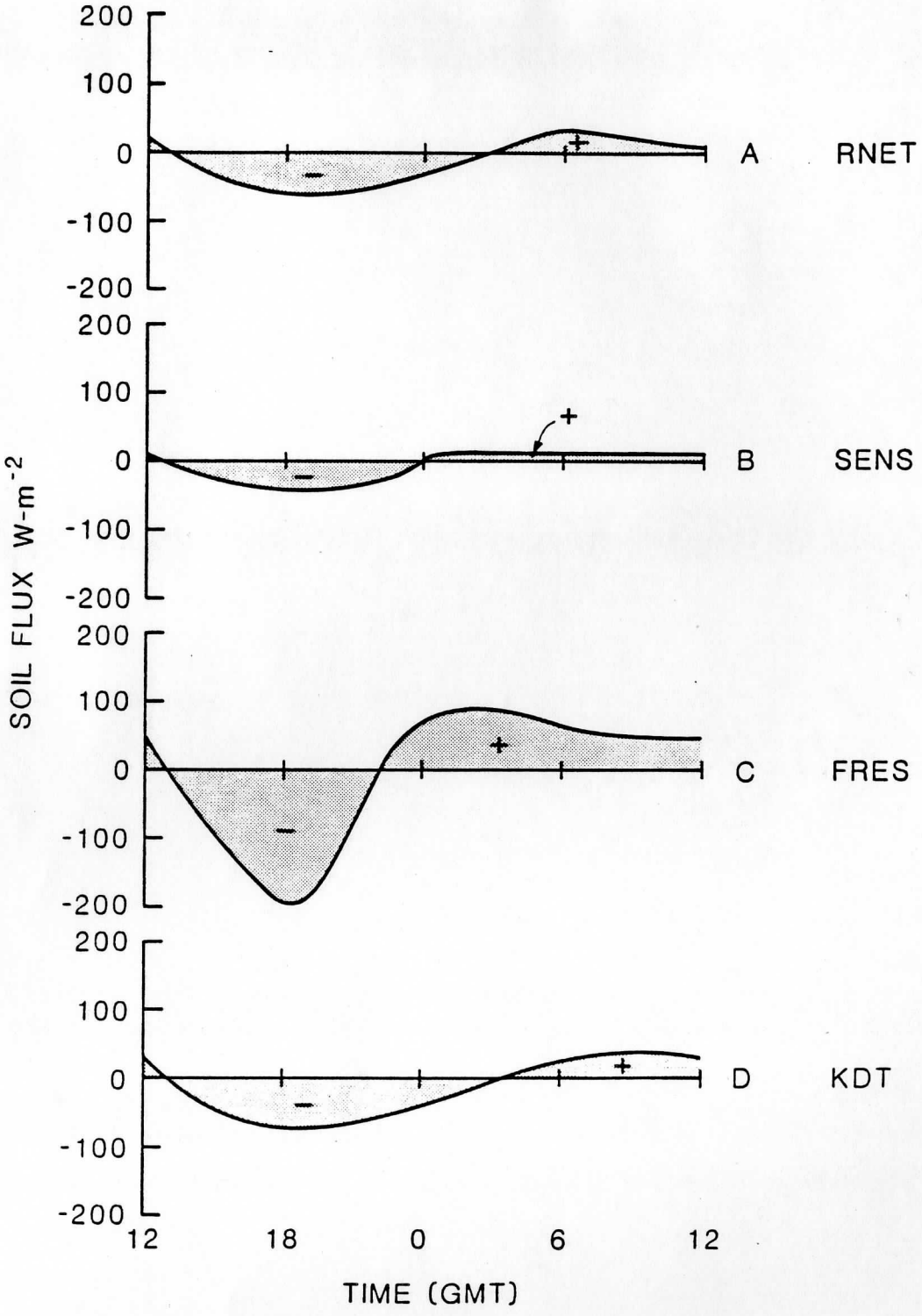
200
100
0
-100
-200
A
RNET
B
SENS
C
FRES
D
KDT
SOIL FLUX W-m-2
12
18
0
6
12
TIME (GMT)

FIG 7

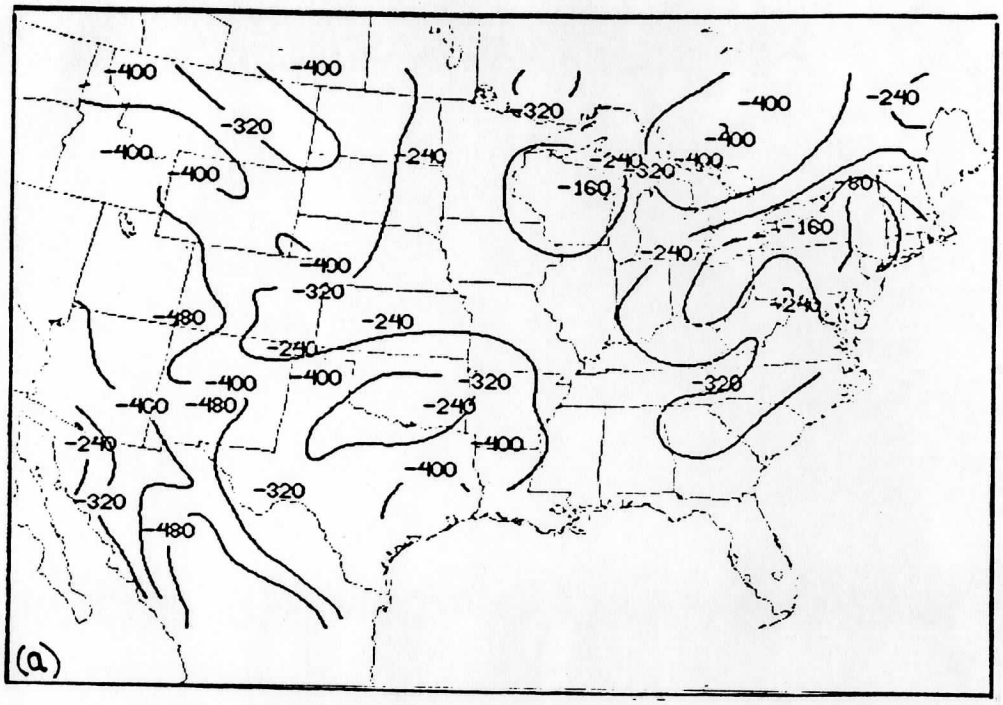
-400
-400
-320
-400
-400
-240
-320
-400
-400
-160
-240
-160
-400
-320
-240
-480
-240
-240
-400
-400
-320
-400
-480
-240
-320
-400
-400
-320
-480
(a)

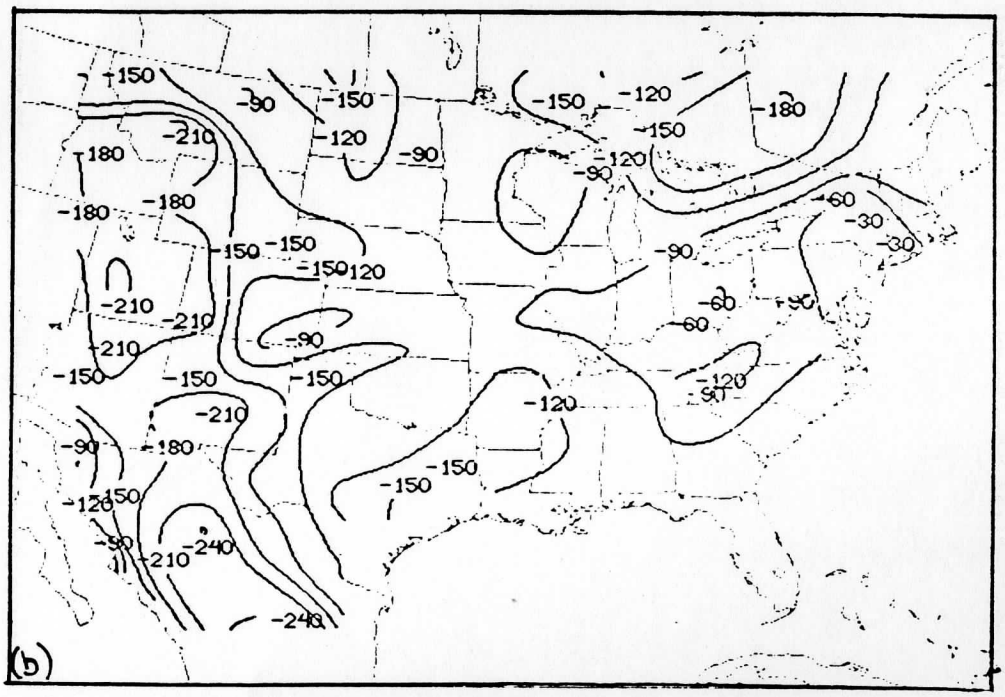
-150
-90
-150
-150
-120
-180
-210
-120
-150
-120
-90
-90
-180
-180
-60
-30
-30
-150
-150
-150
-90
-120
-210
-210
-60
-90
-210
-90
-60
-150
-150
-150
-120
-120
-210
-90
-180
-150
-150
-120
-240
-210
-240
(b)

FIG 8

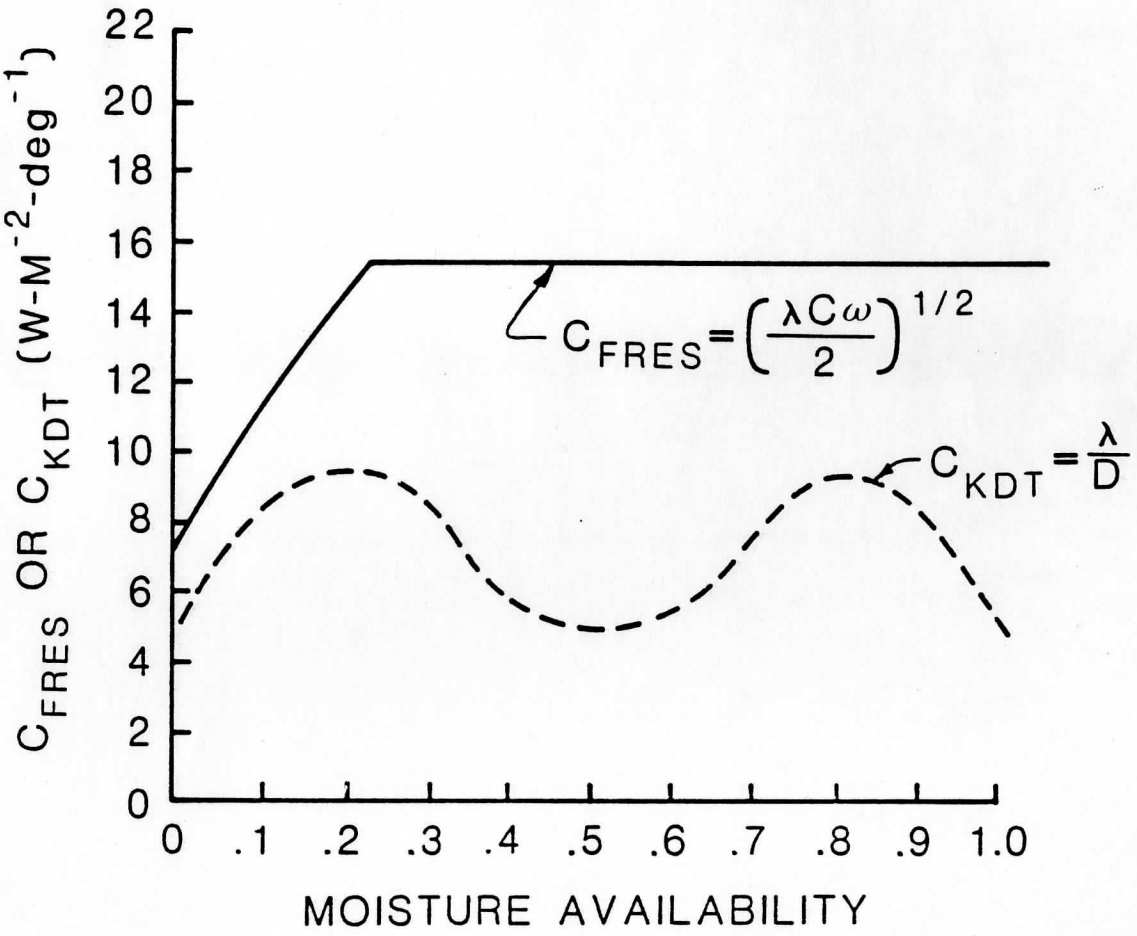
C_{FRES} OR C_{KDT} (W-M^{-2}-deg^{-1})
22
20
18
16
14
12
10
8
6
4
2
0
$C_{FRES}=\left(\frac{\lambda C\omega}{2}\right)^{1/2}$
$C_{KDT}=\frac{\lambda}{D}$
0 .1 .2 .3 .4 .5 .6 .7 .8 .9 1.0
MOISTURE AVAILABILITY

FIG 9

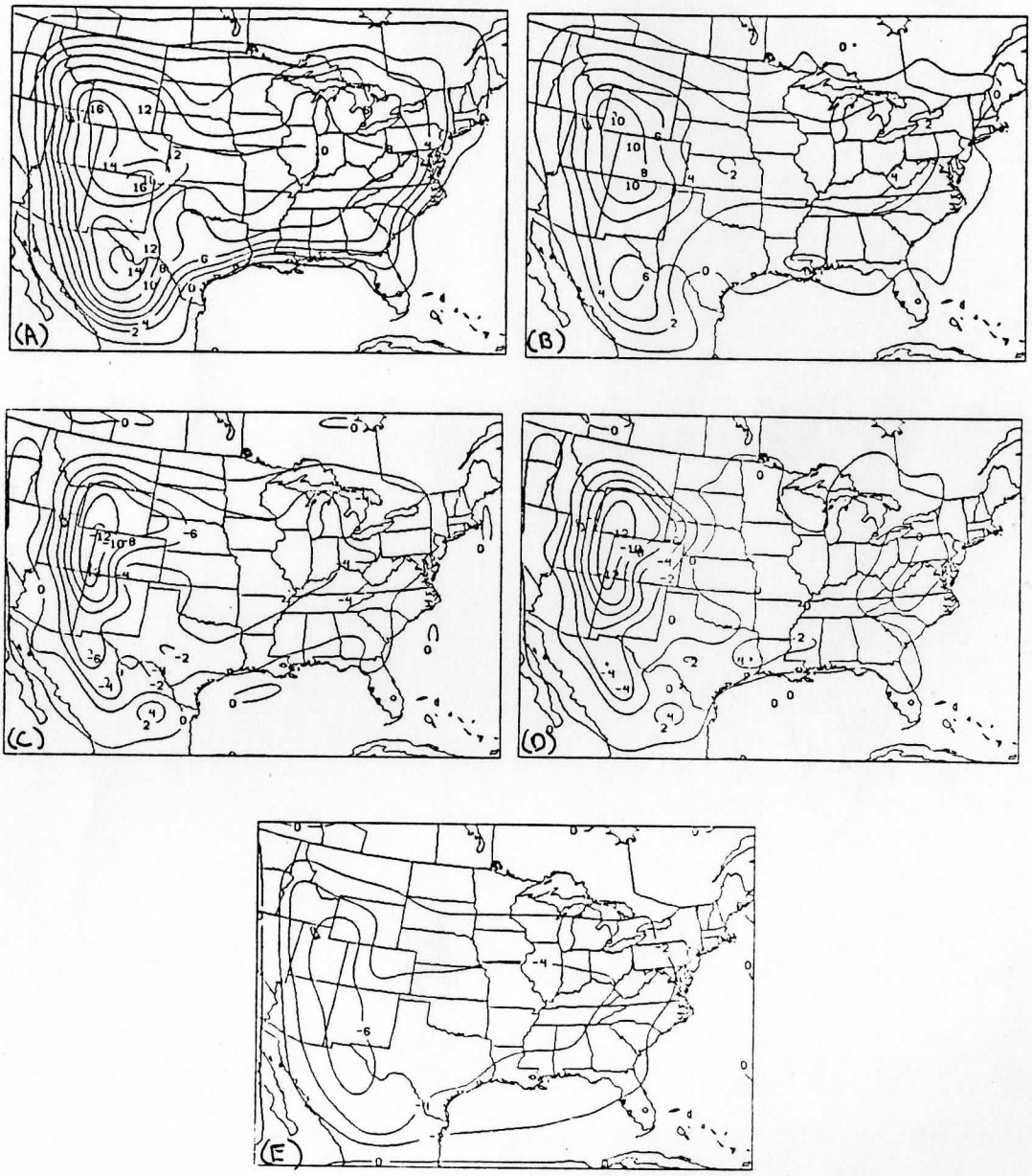

FIG 10

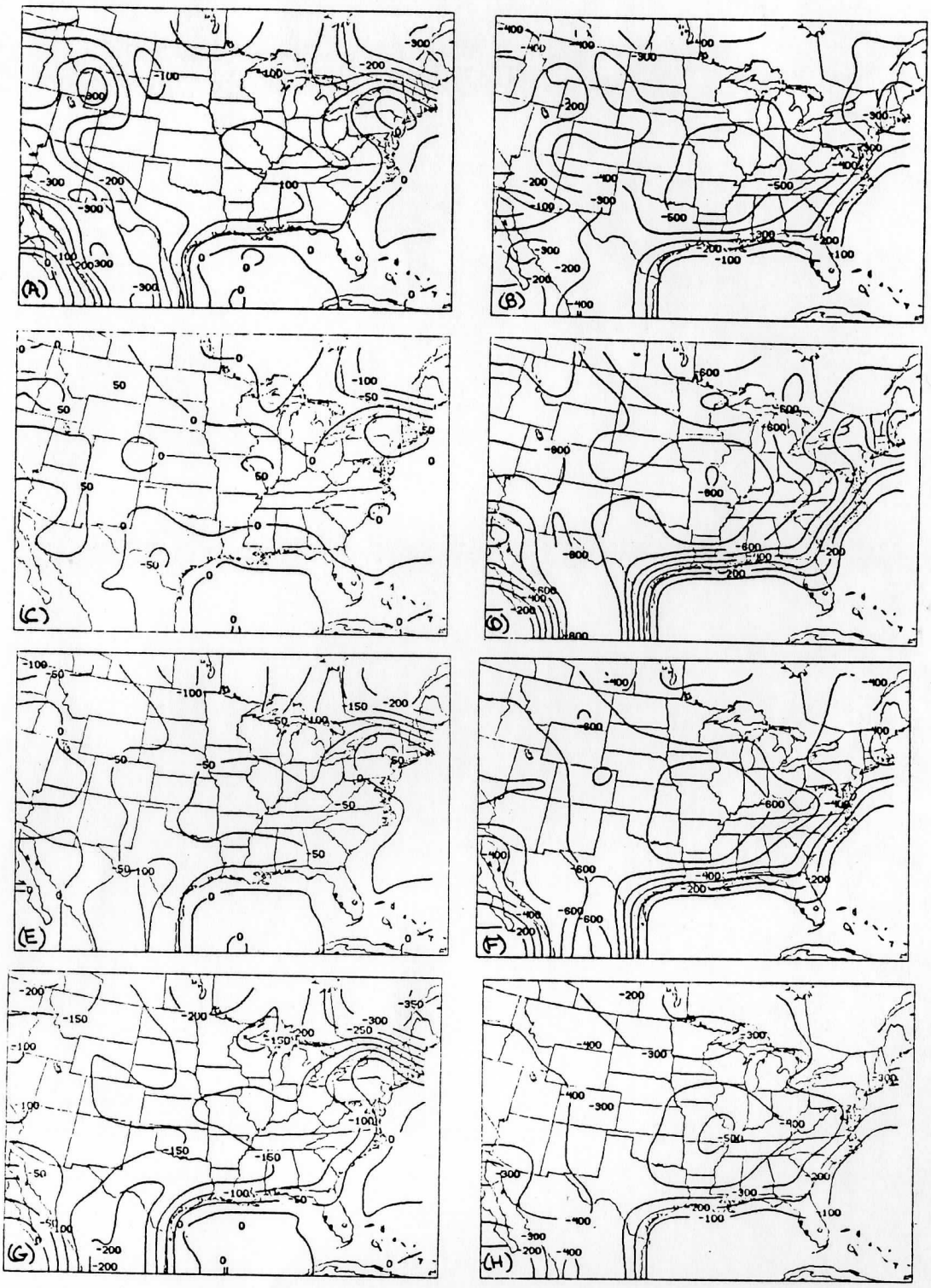

FIG 11

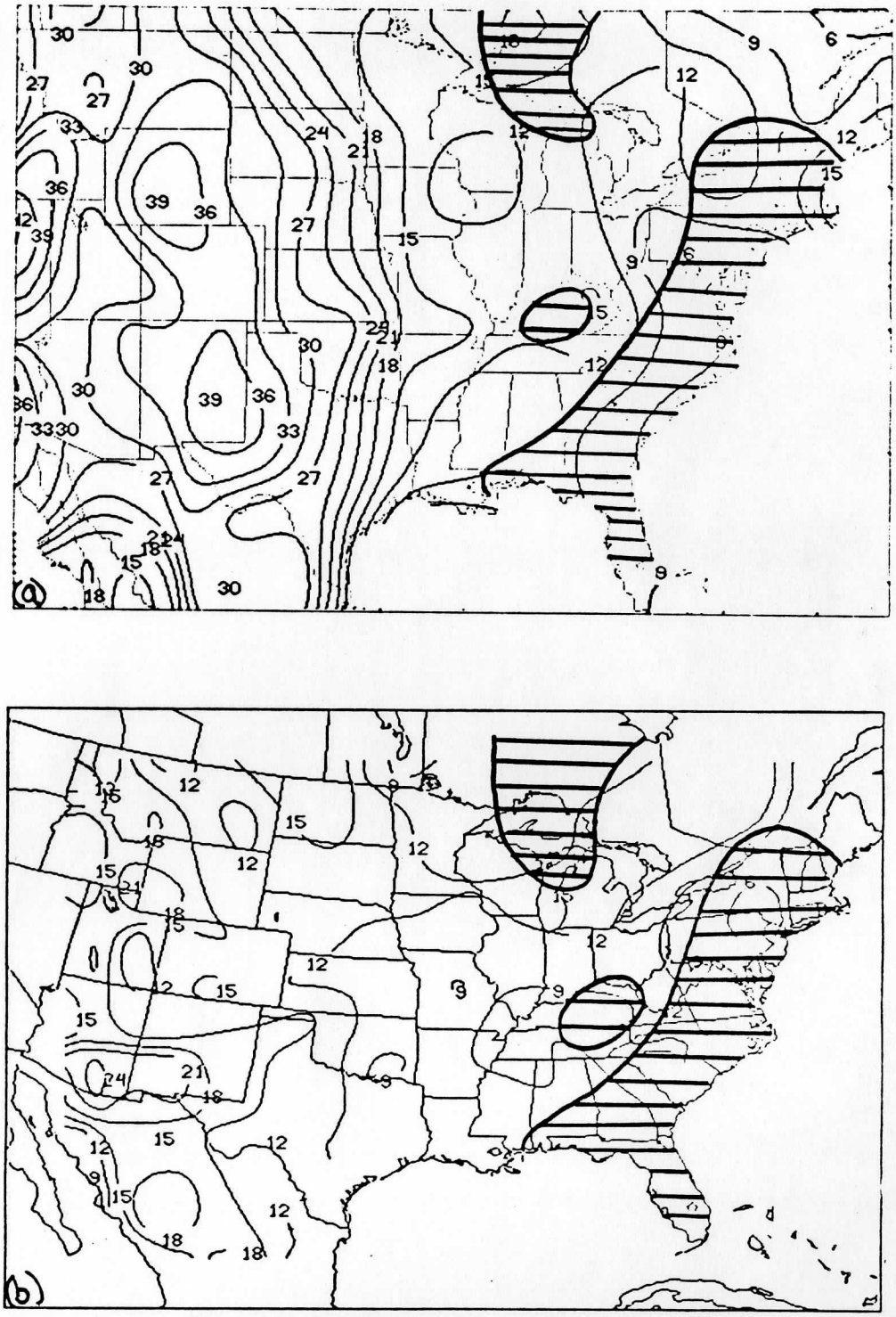

FIG 12

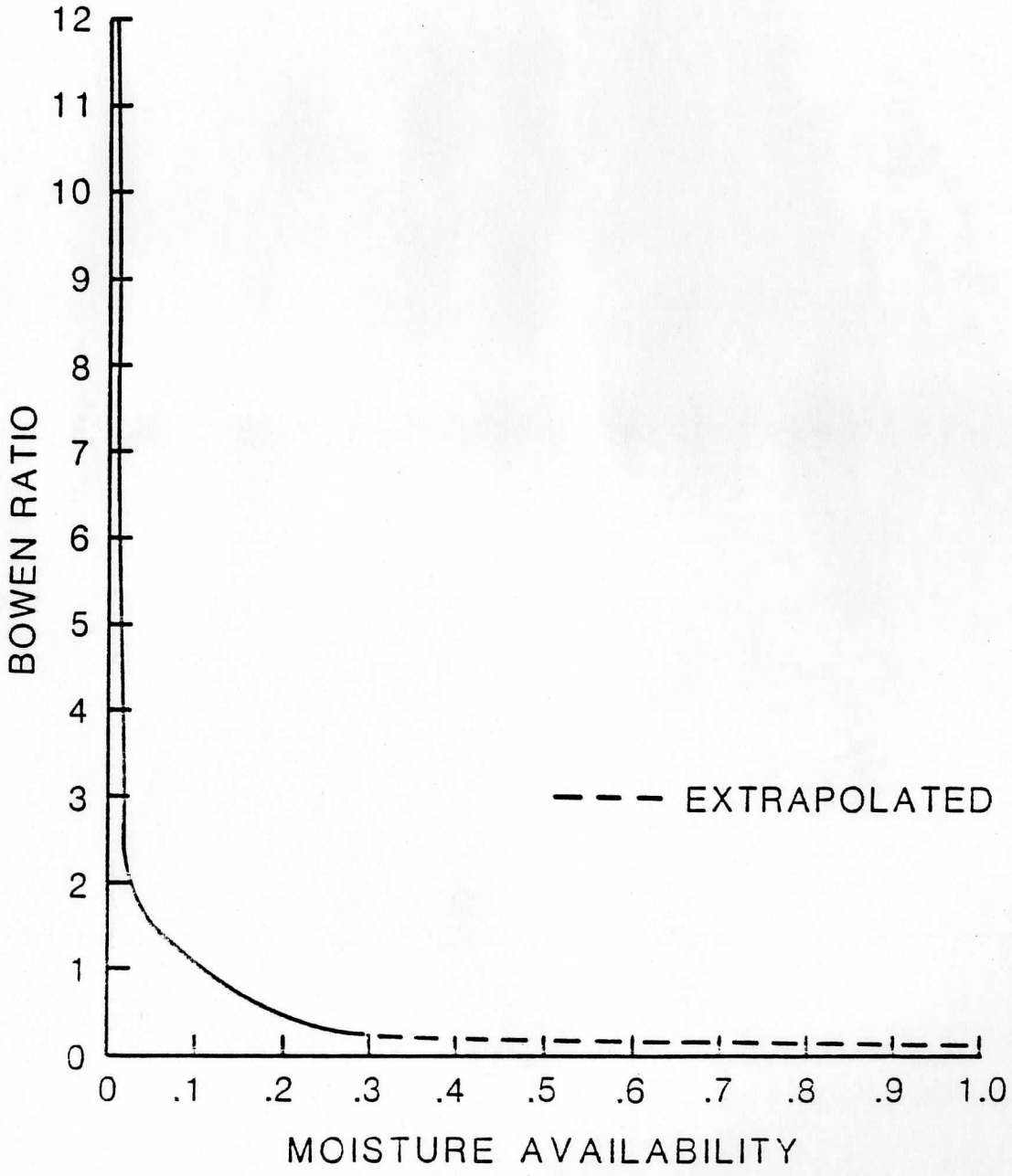
12
11
10
9
8
7
6
5
4
3
2
1
0
BOWEN RATIO
EXTRAPOLATED
0
.1
.2
.3
.4
.5
.6
.7
.8
.9
1.0
MOISTURE AVAILABILITY

FIG 13

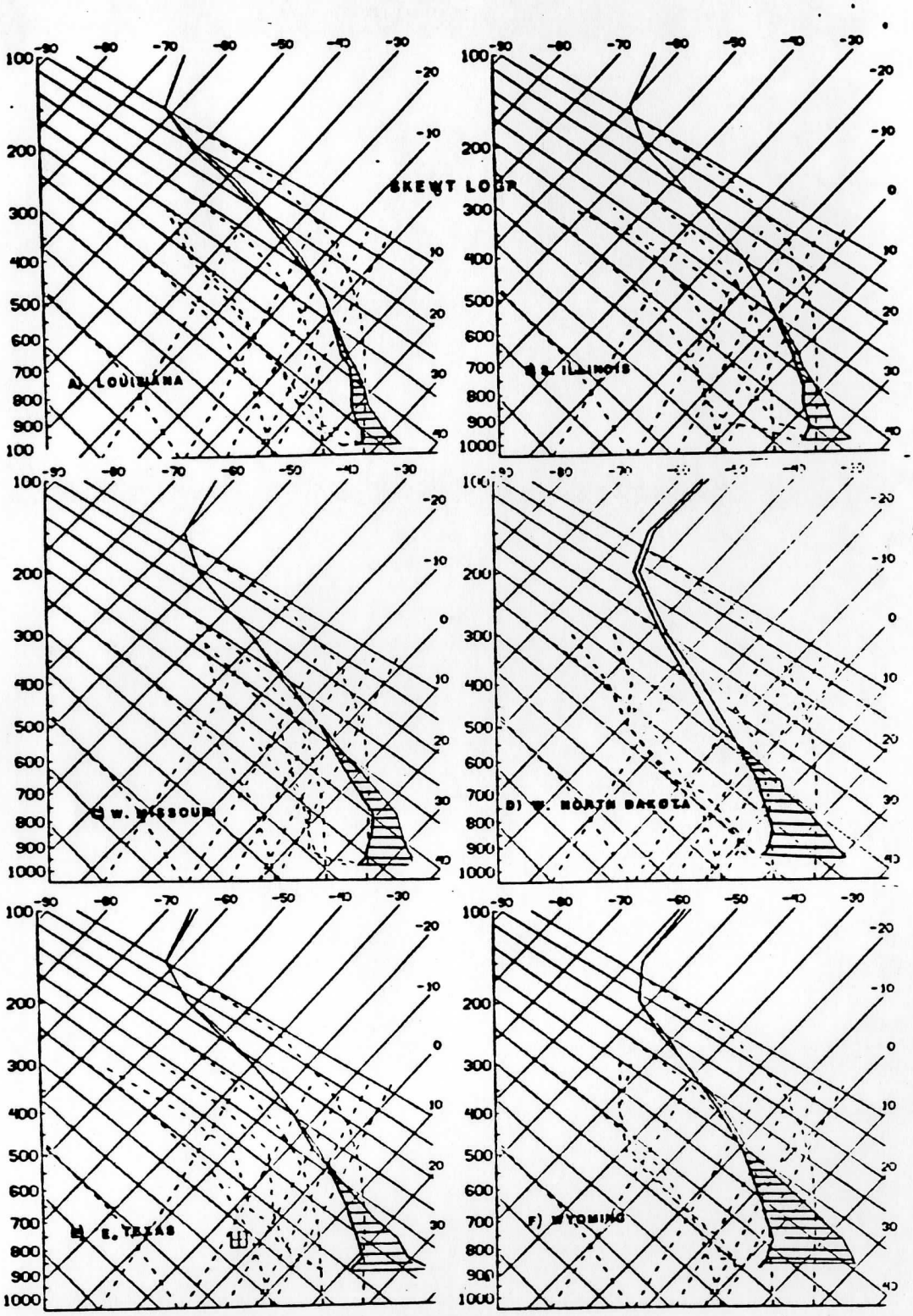
SKEWT LOGP
A) LOUISIANA
B) S. ILLINOIS
C) W. MISSOURI
D) W. NORTH DAKOTA
E) E. TEXAS
F) WYOMING

FIG 14

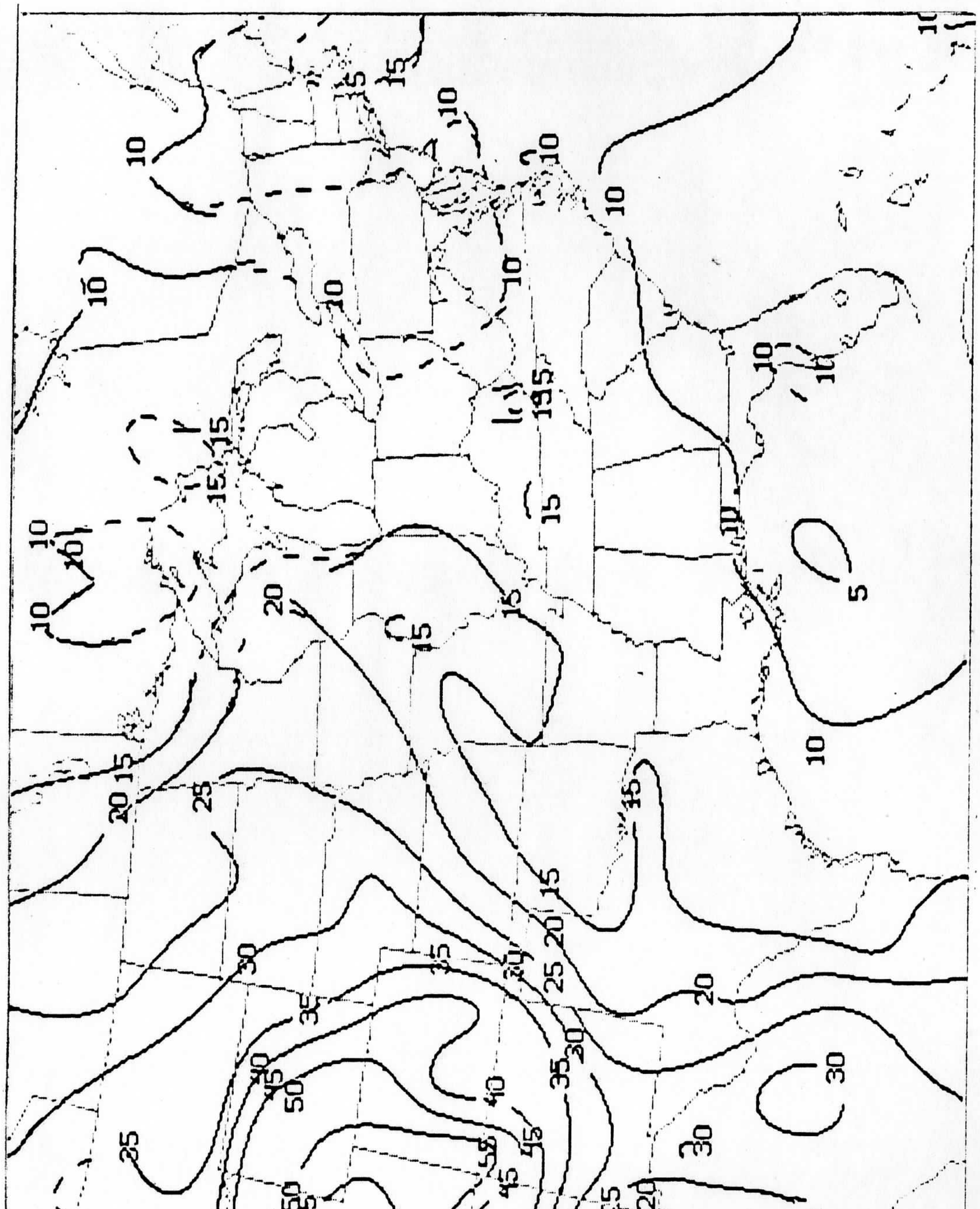

FIG 15

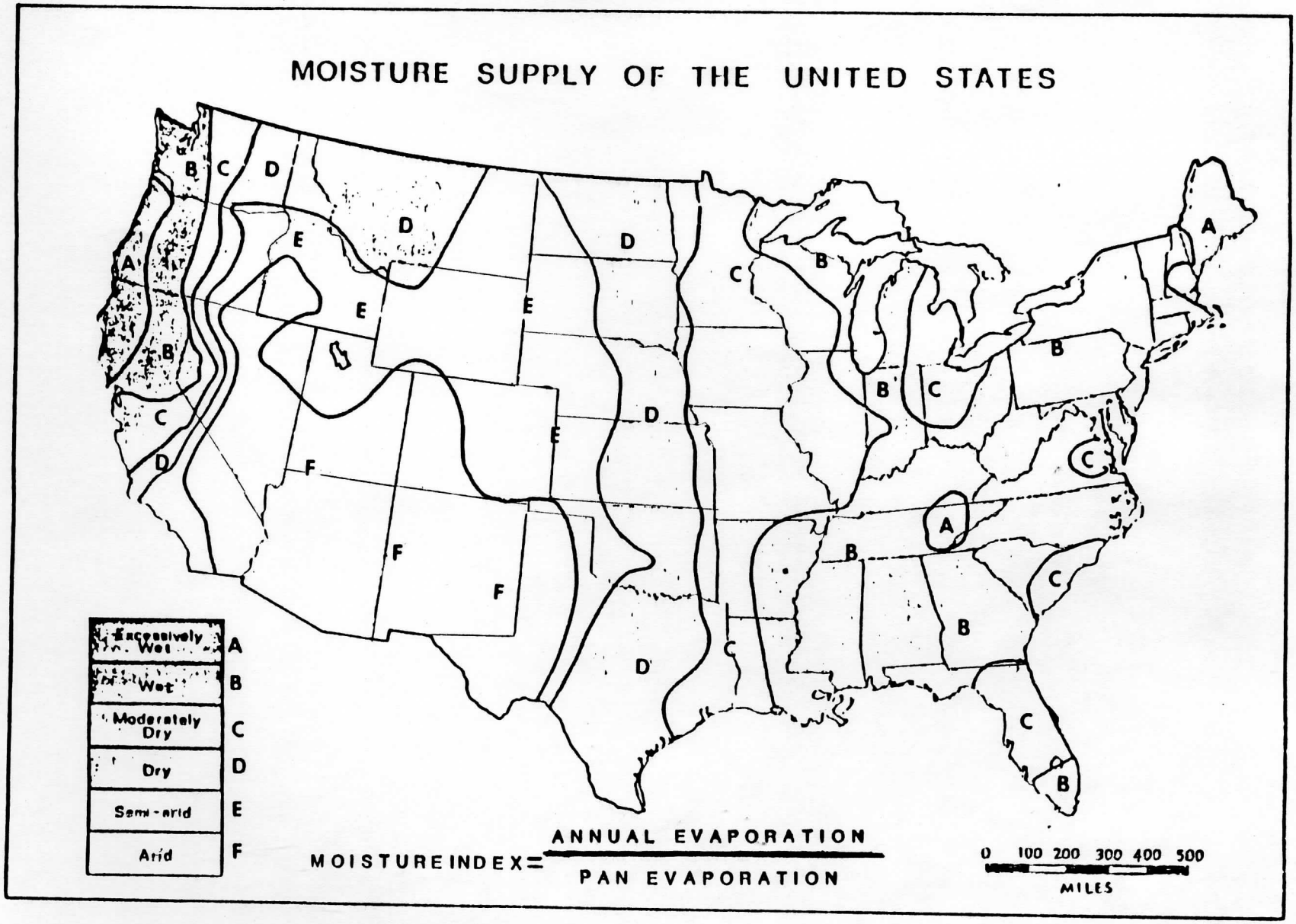
MOISTURE SUPPLY OF THE UNITED STATES
Excessively Wet
Wet
Moderately Dry
Dry
Semi-arid
Arid
A
B
C
D
E
F
MOISTURE INDEX = ANNUAL EVAPORATION / PAN EVAPORATION
0 100 200 300 400 500
MILES

FIG 16

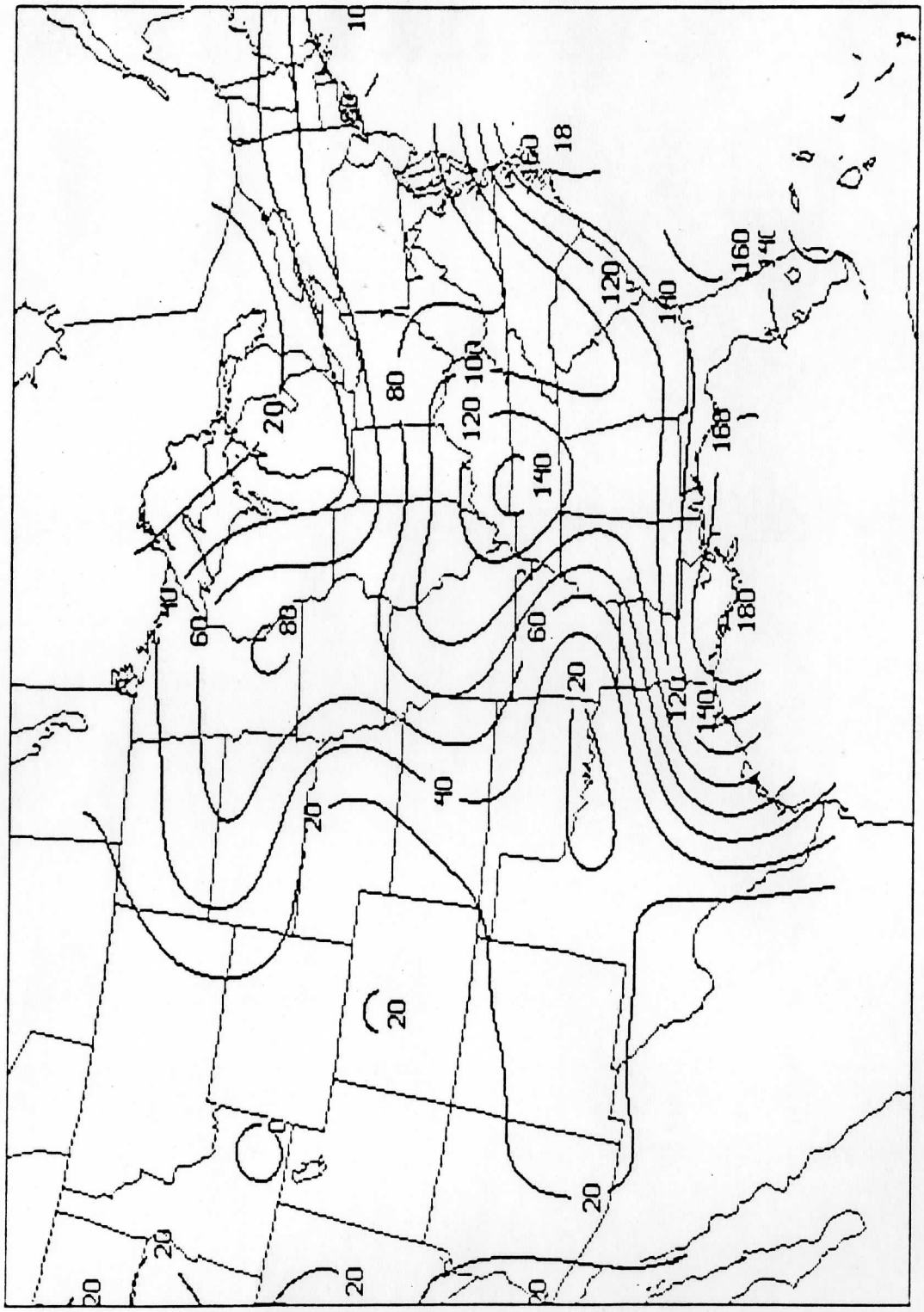
10
18
160
120
140
100
80
120
140
160
180
40
60
80
60
20
120
140
40
20
20
20
20
20
20
20

FIG 17

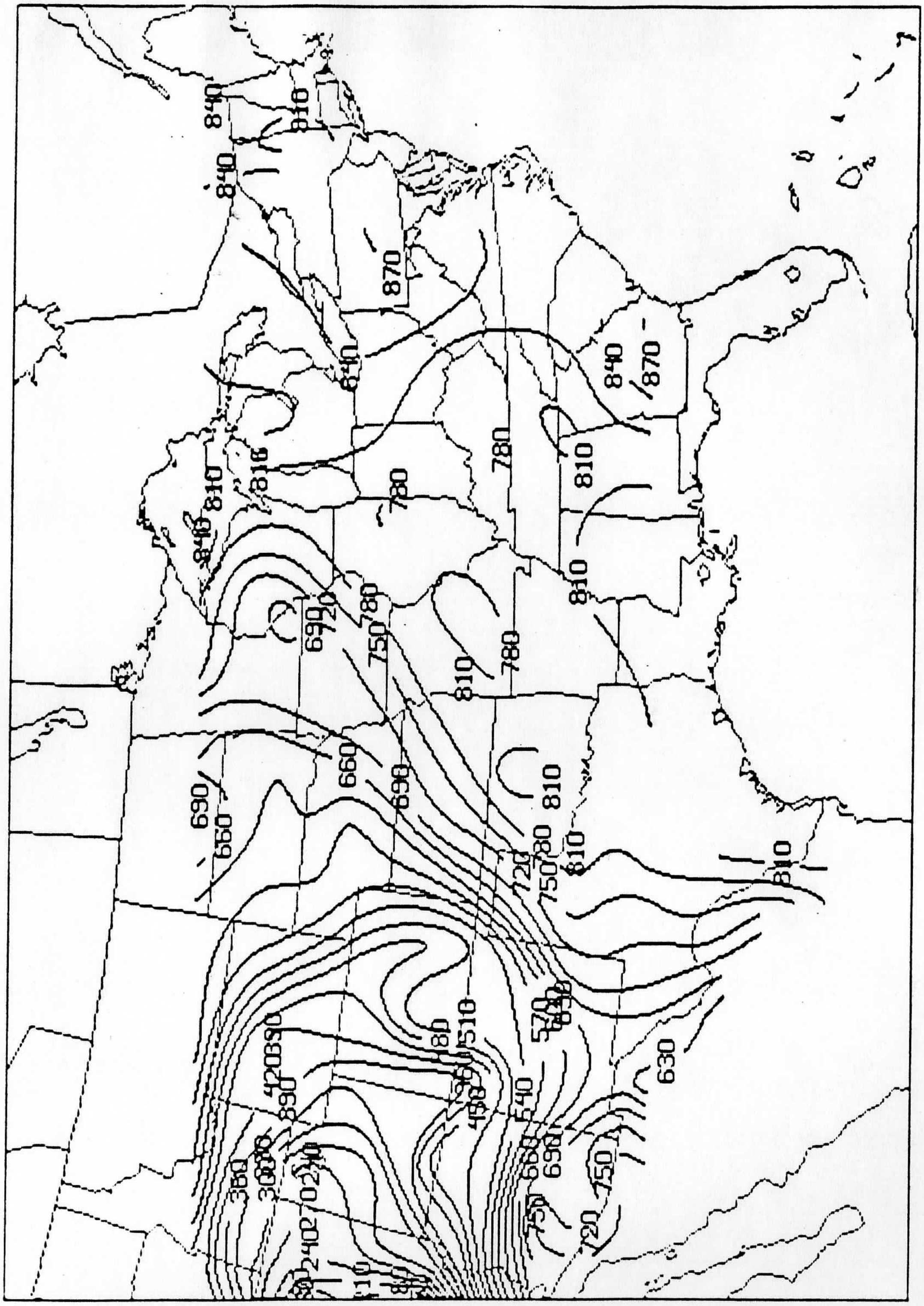

FIG 18

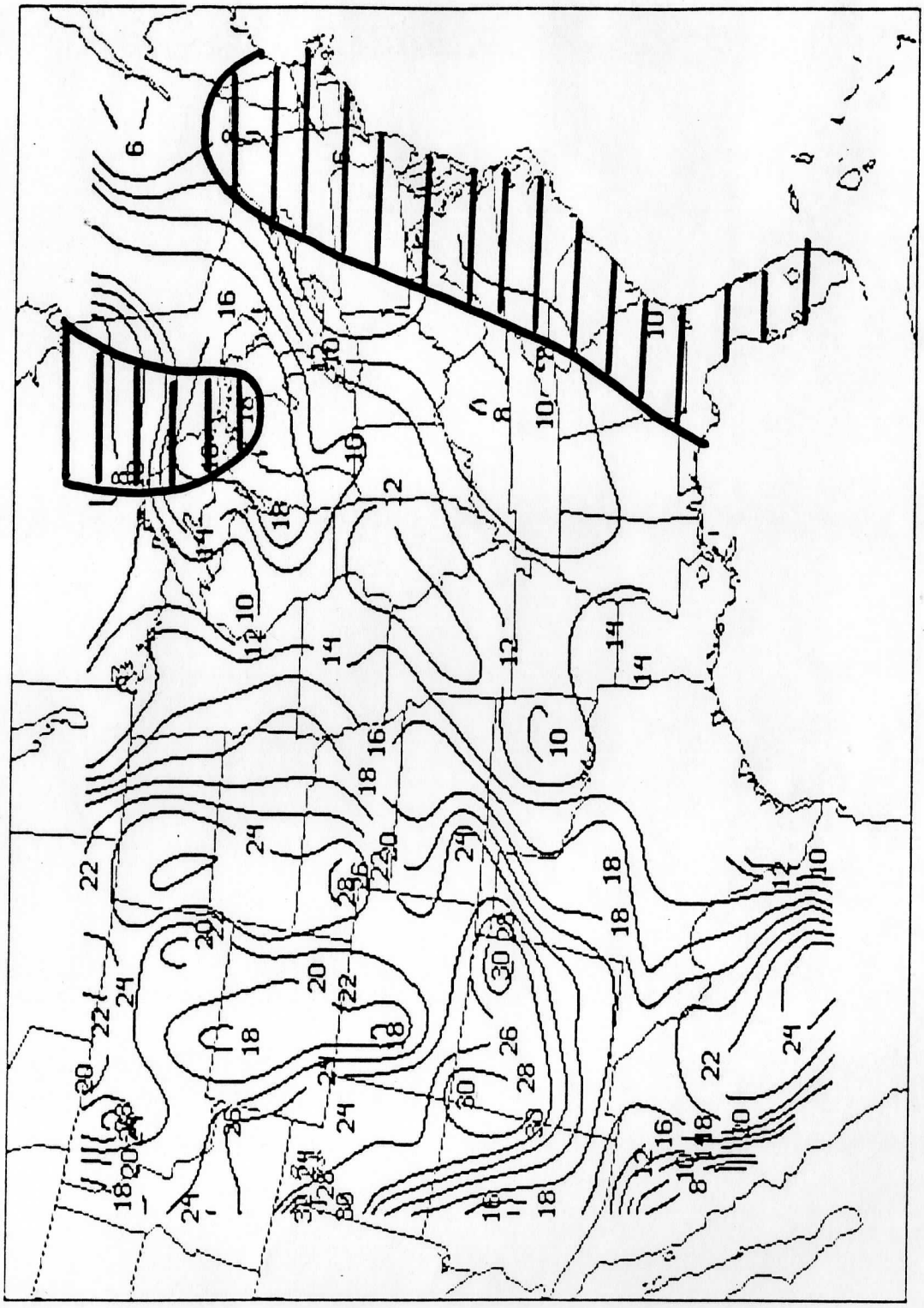

FIG 19

Table 1
Prognosis Model Characteristics

Primitive equations model in σ-coordinates
Ten vertical levels at σ = .09, .19, .29, ..., .99
Horizontal resolution: 134 km
Staggered horizontal grid (Arakawa "C" grid)
Semi-implicit time differencing (Δt = 10 min)
Similarity theory surface layer
Stability dependent vertical diffusion of momentum, heat, moisture above surface layer through depth of PBL
Surface shortwave and longwave flux modified by cloudiness
Surface energy balance equation
Large-scale precipitation
Kuo-type convective parameterization
Horizontal diffusion of momentum, heat, moisture
Updated boundary conditions

Table 2

Forecast Length	Experiment				
	KDT	FRES	RNET	SENS	NOCOND
6 hrs	1.5	1.5	1.5	1.5	1.5
12 hrs	17.2	16.1	16.4	17.0	17.8
18 hrs	51.7	50.5	50.6	50.8	55.8
24 hrs (total)	90.3	83.0	86.5	92.3	103.3

Table 3

Forecast Length	Experiment				
	NOM	GW0	GW.2	GW.5	GW1
6 hrs	1.5	1.6	1.5	1.5	1.4
12 hrs	16.1	18.2	16.1	14.3	18.3
18 hrs	50.5	99.2	48.4	50.6	57.0
24 hrs (total)	83.0	353.8	81.5	85.7	94.6

Table 4

Forecast Length	Experiment		
	NOM	$Z_0.1$	$Z_0 10$
6 hrs	1.5	1.4	1.4
12 hrs	16.1	9.3	10.7
18 hrs	50.5	24.4	34.8
24 hrs (total)	83.0	41.4	63.5